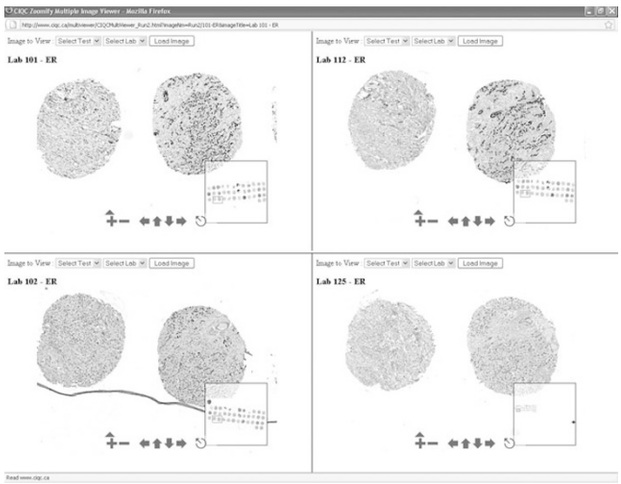

Results: High average observed agreement, sensitivity, and specificity in ER, PR, and HER2 testing was observed (all > 90%). Kappa values were within the target range (> 0.8, or "near perfect" agreement) for all participating laboratories except the following: 1 laboratory for ER, 6 laboratories for PR, and 1 laboratory for HER2. Kendall's coefficient of concordance between the 18 laboratories was 0.942 for ER, 0.930 for PR, and 0.958 for HER2. False positive and false negative results could be identified as either interpretive or technical errors.
Conclusions: The first Canadian IHC EQA testing for ER, PR, and HER2 showed very high concordance between laboratories. The anonymous participation and unrestricted full access provides a means for rapid insight into technical or interpretive deficiencies, allowing appropriate corrective action to be taken.

1665 Use of Formal Root Causes Analysis of Anatomic Pathology Errors to Classify System and Active Components

JB Thomison, H Currens, SS Raab. University of Colorado Denver, Aurora, CO.
Background: Anatomic pathology error evaluation and root cause analysis historically has focused on the misdiagnoses of unusual entities or diagnostic pitfalls for more common diseases, suggesting that error cause is associated with cognitive or performance deficiencies of specific pathologists or clinicians. We evaluated the effectiveness of formal root cause analysis to determine the frequency of specific causes in errors detected by the cytologic-histologic correlation process.
Design: We examined 50 consecutive cytologic-histologic correlation-detected errors in 34 gynecologic and 16 non-gynecologic specimens over a 3 month interval. initially, we used a method that graded discrepant histologic and cytologic specimens in terms of quality and the amount of tumor. We then performed a modified Eindhoven method of root cause analysis to determine latent (system) and active (personnel) causes of error. These causes were then evalauted to examine which error causes could be addressed by process improvement.
Results: In our initial assessment, 48% of cytology/surgical specimens were of low quality consisting of the relative absence of tumor cells, obscuring blood, or other artifacts that limited interpretation. In 33% of these cases, some reviewers retrospectively identified possible tumor although generally classified the sample as non-definitive. Of cases in which the specimen was of sufficient quality, at least some tumor cells were identified in 78% of cases and generally was of low volume. The overwhelming cause of error was multiple system failures. Laboratory sources of error included poor preparation (40% of cases), lack of standardized criteria for classifying specimens as less than optimal (50%), lack of training in the interpretation of challenging samples (60%), and lack of protocols to handle small samples (10%). Clinical sources of error included inadequate handling of bloody samples (30%), lack of clinical standardization in obtaining samples (100%), inexperience, and inadequate transport techniques. Although redesign could address many of these factors, overall systems that resulted in busy schedules, lack of a patient safety focus, and inadeqaute training in improvement techniques hampered actual reorganization.
Conclusions: Pathology errors are almost always multifactorial and results from defective laboratory and clinical systems. Although there is a tendency to attribute error to personnel failures, 100% of individual diagnostic errors occur when systems do not address a vast array of error-prone processes and protocols.

1666 A Cost Efficient Strategy for Deeper Levels on Skin Specimens

AL Wilson, B Nash, WG Watkin. Evanston Hospital, NorthShore University HealthSystem, Evanston, IL.
Background: The optimal number of levels to perform on skin biopsy specimens to reduce turnaround time and minimize cost has yet to be determined. In a previous study, we found that small specimen size (0.5 cm or less), punch biopsies, and those with a clinical impression of cancer or dysplasia were more likely than other specimen types to require deeper levels to arrive at a final diagnosis. In this study we examine a strategy aimed at optimizing efficiency in the handling of skin biopsy specimens.
Design: 199 consecutively accessioned skin biopsy specimens which measured 0.5 cm or less or were punch biopsies formed the study group. These samples were cut prospectively at 4 levels. The control group consisted of 277 skin specimens meeting the same criteria from our 2005 study which were cut at a single level. We compared the turnaround time for the two groups. We also performed a cost analysis comparing this targeted method with prospectively cutting deeper levels on all skin specimens.
Results: In the study group, 13/199 (6.5%) cases required additional levels. The same group of specimens in our prior study in which a single level was performed had a significantly higher requirement for deeper levels, 167/277 (60%) ($p<0.0001$). The turnaround time between the study cases and controls was also significantly different (mean =1.31 days vs. 2.83 days, respectively, $p<0.0001$). Accounting for the initial production of slides and the cutting of additional levels, the projected cost of performing prospective deeper levels on skin specimens measuring <=0.5 cm or punch biopsies is $2.18 less per case than performing prospective deeper levels on all skin specimens. For our hospital, with an average of 20,000 skin specimens a year, this amounts to saving $33,689 per year, or approximately one half of a full time employee equivalent (histotechnologist). Additionally, the projected number of slides for one year cutting selective levels on all specimens is 77,051 vs. 114,077 with prospective levels, resulting in decreased storage requirements.
Conclusions: Cutting prospective deeper levels on skin specimens which measure <=0.5 cm and punch biopsies significantly reduces the need for additional levels and greatly improves turnaround time. Targeting this select group of specimens for prospective deeper levels is more cost effective than performing deeper levels on all skin specimens and reduces storage requirements.

Special Category - Pan-genomic/ Pan-proteomic Approaches to Cancer

1667 Quantitative Assessment of Change in Protein Phosphorylation as a Function of Ischemic Time before Formalin Fixation

Y Bai, A Gopinath, S Siddiqui, H Cheng, E Pectasides, RL Camp, DL Rimm. Yale Universtiy School of Medicine, New Haven, CT.
Background: Post-translational modifications and especially phosphorylation has been shown in preclinical studies to be an excellent method of signaling pathway activation and predicting response to targeted therapies. However, there is evidence that phospho-proteins are dephosphorylated as a function of ischemic time prior to fixation, as is seen in routine processing of surgical pathology specimens. Core Needle Biopsies (CNBs) are typically very rapidly fixed. Here we use this conventional difference in ischemic time to determine the effect of delayed fixation on phospho-specific markers of pathway activation.
Design: Two series of matched CNBs and resections were collected. In series one, 20 cases were examined as a tissue microarray where each specimen was examined in two fold redundancy. The TMA was analyzed by the AQUA® method of immunofluorescent analysis using antibodies to Ki67, p53 and Estrogen Receptor (ER) as controls and antibodies to phospho-Erk (p-ERK), phospho-AKT(p-AKT) and phospho-tyrosine (p-tyr) as the test set. The second cohort was analyzed as whole sections where between 5 and 29 20x fields were assessed on each tissue with an antibody to phospho-AKT.
Results: Both ER and p53 as assessed on the TMA cohort showed no overall trend toward decreased or increased expression in the core biopsy vs the resection specimen. However p-AKT, p-ERK, p-tyr and Ki-67 all showed lower expression in resection specimens. To rule out TMA sampling artifact, whole sections were assayed with an average of 12 and 19 fields for biopsies and resections respectively. In each case, there was consistently and significantly lower levels of pAKT in the resection than in the biopsy (Wilcoxon Signed-Ranks test $p=0.0069$).
Conclusions: This study shows that phospho-proteins are present at decreased levels as a function of ischemic time. This pattern is seen in both TMAs and whole sections. Surprisingly, Ki67 also shows this trend, which could have implications for its use in evaluation of efficacy of neoadjuvant therapy. CNBs appear to be the preferred method for analysis of phospho-proteins for use as a predictor for pathway activation and to assess response to targeted therapies.

1668 Genomic Identification of Biomarkers of Behavior of Pancreatic Endocrine Tumors

J Bauersfeld, DG Thomas, R Kuick, M Vinco, D Sanders, TJ Giordano. University of Michigan, Ann Arbor, MI.
Background: Endocrine tumors of the pancreas are difficult to classify into benign and malignant categories, and as such are often diagnosed as pancreatic endocrine tumors (PETs). The recent WHO classification has improved this situation, but there is still a need for additional molecular biomarkers to provide independent assessment of the risk of malignant behavior.
Design: To identify potential biomarkers of malignant behavior, genome-wide transcriptional profiles were generated for a cohort of 45 PETs using commercially available DNA microarrays. PETs analyzed represented sporadic and syndromic (MEN-1) forms, and primary metastasizing and non-metastasizing tumors, and metastatic tumors.
Results: Using F-tests and selection criteria of $p<0.01$ and fold change > 1.5 in either direction, comparison of 8 PETs with proven metastases (PET-M) to 6 PETs without metastases (PET-N) yielded 255 unique genes whose expression was increased in the PEN-M group and 142 unique genes whose expression was decreased in the PEN-M group. Differentially expressed genes included genes related to tumor invasion and metastasis, as well as other biological processes. Preliminary results from immunohistochemical and AQUA-based validation for several of these biomarkers using tissue arrays containing an independent set of PETs are promising and ongoing.
Conclusions: Genomic investigation of pancreatic endocrine tumors will yield novel biomarkers that will permit a more refined assessment of their risk of malignant behavior. Application of these biomarkers to pathology practice will improve the management of patients with PETs.

1669 Discovery of Molecular Subtypes in Leiomyosarcoma through Integrative Molecular Profiling

AH Beck, CH Lee, DM Witten, S Zhou, K Montgomery, R Tibshirani, T Hastie, RB West, M Van de Rijn. Stanford University Medical Center, Palo Alto, CA; Vancouver General Hospital, Vancouver, BC, Canada; Stanford University, Palo Alto, CA.

Background: The molecular pathogenesis and heterogeneity of soft tissue leiomyosarcoma (LMS) are poorly understood. We employed integrative molecular profiling to characterize molecular subtypes of LMS.

Design: Gene expression profiling was performed on 51 LMS cases using 44k cDNA arrays. Unsupervised clustering was performed to identify subclasses of LMS, and the protein expression of 6 differentially expressed genes was assessed on 3 LMS tissue microarrays (n=425). Array comparative genomic hybridization (aCGH) was performed on 44k arrays for 20 LMS cases. Sparse canonical correlation analysis was performed to identify sets of copy number changes that show significant correlation with sets of gene expression changes. Connectivity map analysis (CMAP) was performed to identify drugs that induce patterns of gene expression inversely correlated with that seen in the LMS subtypes.

Results: Unsupervised clustering demonstrates 3 LMS clusters, which show a high degree of reproducibility (Median In-Group Proportion=1 and $p = 0.05$, following 100 iterations of the clusterRepro algorithm). The clusters show differential expression of multiple gene classes, including genes involved in smooth muscle differentiation. Cases from the muscle-enriched cluster show increased copy number alterations ($p=0.03$), with the majority of cases showing gain at Xp22, 7q31, 3q13, and loss at 1p36 and 16q24 (FDR= 0.016). Sparse canonical correlation analysis performed by chromosome shows that copy number changes in chromosomes 2, 12, and 15 each show significant correlation ($p \leq 0.05$) with sets of gene expression changes. Immunohistochemistry is performed for 6 markers that were highly expressed in the muscle-enriched cluster (ACTG2, CASQ2, SLMAP,ELF1,MYLK,PRUNE2) and demonstrates strong expression of the majority of the proteins in 25% of cases, no strong expression of any of the markers in 35% of cases, and intermediate expression in 30% of cases. The CMAP demonstrates that the 3 LMS clusters defined by gene expression analysis show significant negative connectivity with distinct classes of chemotherapeutic agents.

Conclusions: This integrative analysis demonstrates distinct molecular LMS subtypes, provides insight into their pathogenesis, and suggests that they may respond to distinct classes of chemotherapeutic agents.

1670 Molecular Characteristics of Matched Primary Non-Small-Cell Lung Carcinomas (NSCLC) and Metastases to the Brain

E Benedettini, AG Saad, M Loda, LR Chirieac. Brigham and Women's Hospital, Boston, MA; Dana Farber Cancer Institute, Boston, MA; Harvard Medical School, Boston, MA.

Background: Despite recent advances, the molecular mechanisms of brain metastasis remains poorly understood. The design of new targeted, patient-specific therapies requires knowledge of the presence of the molecular abnormalities that are present in both the primary tumor and distant metastatic sites. To determine whether the genetic profiles are constant between the primary lung cancers and their paired metastases we examined pairs of human primary and metastatic lung carcinomas by high-throughput gene mutation profiling.

Design: We evaluated formalin-fixed paraffin-embedded specimens from 21 patients (11 women [52%] and 10 men [48%], median age 65 years) with NSCLC metastatic to the brain and the corresponding primary primary NSCLC and brain metastases using the Sequenom mass spectrometry-based system (iPLEX protocol - OncoMap analysis) for 252 genetic mutations in ABL1, BRAF, EGFR, FGFR3, HRAS, KIT, KRAS, MET, NRAS, PDGFRA, PI3K, and RET. Some of the lower confidence mutations identified by iPLEX protocol were validated by homogeneous mass-extend (hME) technology.

Results: The results of molecular markers expression in the primary NSCLC and in metastatic brain NSCLC are summarized in table 1. In nine patients (39.1%) mutations were identified only in the primary lung tumors, in five patients (21.7%) mutations were identified only in the brain metastases, and in three patients (13%) mutations were identified in both lung and brain metastases. Except KRAS G12C mutation that was identified in two patients, all mutations identified were present in only one patient.

Results of various molecular markers in the primary NSCLC, metastatic brain NSCLC, or both

Gene	Primary NSCLC	Metastatic NSCLC to brain	Present in Both Primary and Brain NSCLC
ABL1	Y253F	G250E	
BRAF	D594G	D594G	D594G (one case)
EGFR	Exon19 del, D770_N771>AGG		
FGFR3		K650T	
HRAS	G13D		
KIT		V559I	
KRAS	G12C	G12S; G12D; G12C	G12C (two cases)
P*DGFRA*	T674I		
PI3K	G1049R		
RET	E632_L633del		

Conclusions: Our results showed that tumors have a great variation in their molecular abnormalities. Understanding the effect of these molecular differences between primary non-small-cell lung carcinomas and metastases to the brain will allow us to clarify the mechanism of metastatic progression of NSCLC to brain and potentially identify novel targets of therapy.

1671 High-Throughput Immune Receptor Sequencing for Diagnosis, Prognosis and Monitoring of Lymphoid Malignancies

SD Boyd, JD Merker, JL Zehnder, AZ Fire. Stanford University, Stanford, CA.

Background: High-throughput DNA sequencing methods offer new approaches to analysis of rearranged immunoglobulin (Ig) and T cell receptor (TCR) loci in suspected lymphoid malignancies. Sequencing provides much more complete characterization of the receptor rearrangements present in a specimen compared to capillary or gel electrophoresis.

Design: Our method uses multiplexed PCR amplification of IgH loci followed by high-throughput pyrosequencing to detect clonal sequences, determine hypermutation status, and test for the presence of low levels of known clonal receptors. We employ physical bar-coding of DNA molecules derived from different samples to enable cost-effective sequencing of sample pools. 23 pooled specimens were sequenced including: 4 known lymphoma specimens; 4 peripheral blood leukocyte samples from healthy individuals; 7 specimens with indeterminate or discordant results by conventional clonality assays; and a dilution series of a clonal CLL/SLL specimen into normal peripheral blood leukocytes.

Results: We obtained 522,099 IgH sequences from the 23 pooled specimens, with a mean read length of 242 base pairs extending from the J segment to the V segment FR2 framework region. Alignment of rearranged IgH sequences to germline V, D and J gene segments using IgBLAST from NCBI are being compared to the results from other algorithms. Clonal IgH populations are readily detected and characterized as to their germline or hypermutated status and unique V-D and D-J junctions with this approach. The components of oligoclonal specimens are evident from the sequence data, and can be identified as distinct rearrangements or subclones related to each other. Clonal receptor sequences can be reliably observed after 1000-fold dilution, suggesting that the method could be used to monitor for residual disease. Healthy peripheral blood specimens show expected extensive sequence diversity. We are exploring methods for optimally summarizing and representing these data.

Conclusions: Newly-available DNA sequencing technologies provide unambiguous data about the diversity and properties of immune receptors present in the B and T cells of a clinical specimen, and could be used as an aid to diagnosis, prognosis, therapeutic monitoring and better understanding of hematopoietic disease. More broadly, extensive sequencing of Ig and TCR rearrangements offers a novel approach to monitoring normal immune responses such as the response of patients to vaccination, and of characterizing the immune system in patients with autoimmune diseases.

1672 Quantitative Immunohistochemistry in the Differential Diagnosis of Lung Tumours with Hierarchical Cluster Analysis and Ranked Comparative Graphic Immunoprofile

B Bozoky, C Fernandez, M Bjornstedt. Karolinska University Hospital, Huddinge, Stockholm, Sweden.

Background: Currently, classification and differential diagnosis of lung tumours is mainly based on their histological features, in absence of a comprehensive immunohistochemical characterisation. This study was aimed to assess and prove the importance of the quantitative immunohistochemical approach as a diagnostic tool in the differential diagnosis of lung tumours.

Design: 285 lung tumours including 157 adenocarcinomas (AC), 37 squamous cancers (SC), 61 neuroendocrine tumours (NT), 19 large cell cancers (LC) and 11 adenosquamous cancers (AS) were immunostained with up to 41 conventional antibodies, semiquantitatively evaluated according to the extent of immunoreactivity (scarce:<10%; partial:10-85%; diffuse:>85%), registered in spreadsheet format and imported into a relational database. This database was used for hierarchical cluster analysis and ranked comparative graphic immunoprofiles (CGIP) for the differential diagnosis. GCIP were generated by a tailored, self developed software application and statistically significant antibodies were calculated using t-test and significance analysis of microarrays (SAM).

Results: Hierarchical clustering analysis separated three main tumour types and related specific antibody clusters: AC-specific set comprising cytokeratin (ck) 7, ck18, ck19, CEA, CA125, TTF1, EMA, Muc1, Muc5ac; SC-specific set including ck5, ck17, HMWck, p63, maspin; and NT-specific set containing CD56, chromogranin A, synaptophysin. AS and LC cancers could only be separated from the main tumour types by ranked CGIP supported by significance analysis. The statistically significant antibodies were determined for the differential diagnostic alternative of: AC-SC, AC-AS, AC-LC, SC-AS, SC-LC, AS-LC and NT against all the other tumour types.

Conclusions: Comprehensive graphic immunoprofiles for the different lung tumour types and antibody clusters specific for AC, SC and NT could be provided. Different sets of antibodies proved to be statistically significant in the differential diagnosis of the five tumour types depending on the diagnostic context. Ranked CGIP can visualize these differences and can be used as differential diagnostic tool.

1673 A Quantitative Multiplex Protein Assay for Analysis of Intracellular Signaling Pathways in Sarcoma Samples

M Bui, W Brazelle, J Gemmer, S Altiok. Moffitt Cancer Center, Tampa, FL.

Background: Patients with advanced metastatic sarcomas have poor prognosis with a disease-free survival at 5 years less than 10%. New and better agents are warranted for the treatment of these diseases. The modern revolution in molecular biology has led to characterization of biologically important signaling pathways in cancer, the elements of which have focused drug development efforts towards novel, targeted therapies, and to identify specific molecular biological profiles for each tumor. The greatest challenge in clinical studies is to identify subgroups of patients who will benefit from different types of targeted treatments. The purpose of this study is to develop quantitative pharmacodynamic assays to predict and assess tumor response to targeted therapeutics in sarcoma patients.

Design: Tumor tissues corresponding to approximately four core biopsy samples were collected from resection samples in accordance with IRB requirements. Cellular extracts were prepared and the expression levels and phosphorylation status of intracellular signaling proteins as well as markers of apoptotic cell death were analyzed in by using the Luminex® xMAP system. The levels of phospho proteins were normalized to their total expression levels.
Results: The quantitative multiplex assays enabled simultaneous analysis of activation status of the extracellular signal regulated MAP kinase (Raf/Mek/Erk), PI3K/Akt and mTOR/p70S6 pathways and of apoptotic protein caspase 3 in as small as 3 micrograms of cellular proteins. Western blot methods corroborated the results of multiplex analysis. The sarcoma cells obtained from patients with spindle cell sarcoma, myxoid chondrosarcoma, synovial sarcoma, myxoid spindle cell sarcoma, osteosarcoma and myxoid liposarcoma showed significant variation in their signaling profiles, suggesting predictor of patient response to targeted therapeutics before the initiation of treatment.
Conclusions: Collectively, these results demonstrate that the components of the signaling pathways can be quantitatively analyzed in sarcoma samples to assess the efficacy of the therapy *in vivo*. This approach may also open the avenues to explore the molecular mechanisms leading to drug resistance in individual patients, which may lead to design of combination therapies to block aberrantly activated pathways in individual patient's tumor. We will apply the methods described here to clinical samples collected from patients with extremity and retroperitoneal sarcomas treated with an mTOR inhibitor in an upcoming clinical trial.

1674 Molecular Pathways Associated with Hormone Refractory *TMPRSS2-ERG* Fusion Prostate Cancer

YB Chen, B Moss, S Banerjee, S Perner, C Lafargue, DS Rickman, K Sircar, TA Bismar, MA Rubin, F Demichelis. Weill Cornell Medical College, New York; MD Anderson Cancer Center, Houston; Univ. of Calgary, Calgary, Canada.
Background: Men with advanced prostate cancer (PCa) often develop an androgen-independent (hormone-refractory, HR) state within months to years of androgen deprivation therapy (ADT). The absence of effective treatment for HR PCa is the main cause of morbidity and mortality and reflects a lack of knowledge on how tumor evades androgen dependency. The role of *TMPRSS2-ERG* fusion in the pathogenesis of HR PCa is unknown.
Design: We analyzed a unique cohort of 59 men with ADT-treated locally advanced or metastatic PCa who were clinically diagnosed as HR when receiving a palliative transurethral resection of prostate (TURP). Gene expression profiling was performed by DNA-mediated annealing, selection, ligation and extension (DASL) using RNA extracted from formalin-fixed paraffin embedded tissue cores from 83 TURP specimens. The custom DASL arrays allowed us to interrogate 6144 informative genes. *TMPRSS2-ERG* fusion status was evaluated by an ERG break-apart FISH assay.
Results: High-quality expression data were obtained from 76 of 83 (91.6%) samples. Expression of genes reported in HR PCa such as AR, FOLH1(PSMA) and AKR1C3 were consistently observed. Principle component analyses did not reveal discrete sample clusters, compatible with the known heterogeneity of HR PCa. Intriguingly, the 87 gene signature of *TMPRSS2-ERG* fusion, previously identified and independently validated in untreated localized PCa cohorts, could not distinguish samples with ERG rearrangement from those without. This suggests ADT has a dominant effect on the expression profile of PCa. Nonetheless, 28 differentially expressed genes were identified between fusion positive vs. negative groups, including 24 up- and 4 down-regulated genes in the positive group. Multiple genes potentially related to steroid hormone processing (SULT1A1) and signaling (PRDM2, SLC39A6, UBE3A) were up-regulated in fusion positive cases. Genes implicated in IGFR, HIF-1, clathrin-dependent endocytic and cytoskeleton regulatory pathways were also differentially expressed depending on the *ERG* fusion status.
Conclusions: Using a novel expression profiling technology, we showed that HR PCa is a heterogeneous group where the ADT effect altered the molecular signature of *TMPRSS2-ERG* fusion seen in localized hormone-naive tumors. Our results suggest tumors harboring the fusion may progress via distinct molecular mechanisms than the fusion negative tumors.

1675 Novel Submicroscopic Genomic Alterations Identified in Diffuse Large B-Cell Lymphoma Using High-Resolution Oligonucleotide-Based Array CGH Analysis

JL Christal, RA Higgins, AR Bolla, RS Robetorye. The University of Texas Health Science Center at San Antonio, San Antonio, TX.
Background: Diffuse large B-cell lymphoma (DLBCL) is the most common type of non-Hodgkin lymphoma and is comprised of clinically heterogeneous groups. This heterogeneity has led to attempts to identify distinct subgroups of DLBCL using immunophenotypic methods, gene expression profiles, and molecular cytogenetic alterations. Here, we report analysis of a total of 85 cases of DLBCLs and DLBCL cell lines using high-resolution oligonucleotide-based array comparative genomic hybridization (array CGH) in order to identify novel recurrent submicroscopic genomic imbalances in DLBCL. These alterations may help to identify genes that have potential clinical and biological signficance.
Design: Fifty-seven nodal and extranodal DLBCLs and 28 DLBCL cell lines were analyzed using Agilent Human Genome 44K CGH oligonucleotide arrays (Agilent Technologies, Santa Clara, CA) according to the manufacturer's recommendations. Slides were scanned with an Agilent Scanner, and the data were analyzed with Agilent Feature Extraction and CGH Analytics software. Array CGH results for each case were also subjected to penetrance analysis to identify common regions of genomic alteration.
Results: Array CGH analysis and penetrance plots identified several previously described genomic regions with frequent copy number alterations in DLBCL, including 1q gain, 2p gain (includes *REL*), 6q loss, 8q gain (includes *MYC*), 9p21 loss (includes *CDKN2A* and *CDKN2B*; Figure 1), and 17p loss (includes *TP53*). However, additional regions exhibited novel recurrent submicroscopic genomic alterations, including gains at 7p22 and 7q22, and losses at 1p36, 2p12, 14q32, 19p13, 19q13, and 22q11.
Conclusions: High-resolution oligonucleotide-based array CGH identified many previously described genomic alterations associated with DLBCL. In addition, several novel submicroscopic genomic alterations of potential importance were identified in these lymphomas. Additional studies will be required to identify relevant genes in these newly identified regions to determine whether alterations in the expression of these genes might play a role in the pathogenesis of DLBCL.

Figure 1. Penetrance analysis of chromosome 9 reveals loss of genomic material on 9p21 (arrow) in 37% of DLBCL cases. This region includes the *CDKN2A* and *CDKN2B* genes.

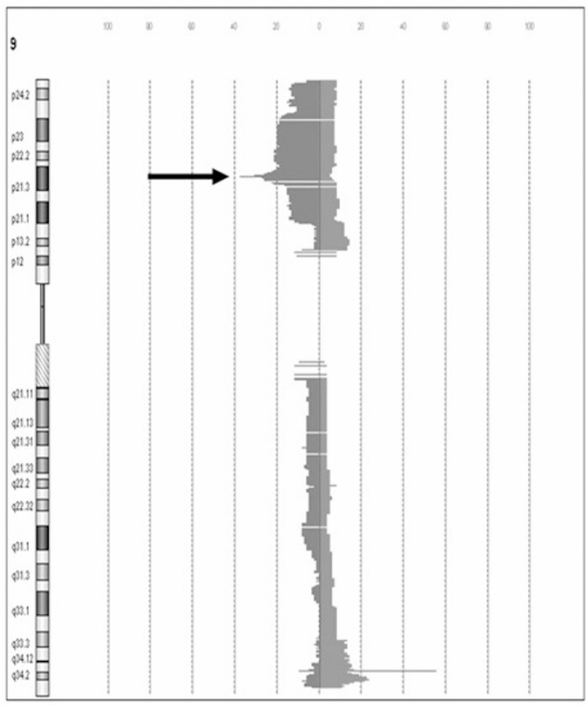

1676 MicroRNA Expression Profiles in Pediatric Precursor T Lymphoblastic Leukemia/Lymphoma

M Czader, K Rizzo, G Vance, A Tewari, S Bhagavathi, J Olczyk, M Nassiri. Indiana University School of Medicine, Indianapolis, IN; University of Miami, Miami, FL.
Background: Precursor T lymphoblastic leukemia/lymphoma (T-LL) represents 15% of newly diagnosed pediatric lymphoblastic leukemias/lymphomas. A significant proportion of cases present with high risk features such as bulky mediastinal mass, high WBC and CNS involvement. Despite improved outcomes due to therapy intensification, T-LL remains a high-risk disease with nearly 30% relapse rate. As further escalation of chemotherapy is not feasible, there is a need to optimize classification for improved treatment assignment and outcome prediction. To further study biological diversity of T-LL, we have investigated microRNA (miRNA) expression profiles in a series of T-LL patients. The role of miRNAs is related to targeting mRNAs encoding oncogenes and tumor suppressor genes. The association of miRNA profiles with clinicopathological variables and patient outcome has not been studied in T-LL.
Design: Thirty eight cases of T-LL were studied (bone marrows and lymph nodes). Median patient age was 9 years. There were 32 males. The median WBC at presentation was $23.3x10^9$/L (range $2.5-945x10^9$/L). The majority of patients had mediastinal mass and/or lymphadenopathy. Microarray studies were performed using Agilent human miRNA microarrays (version 2.0) containing 723 human and 76 human viral miRNAs cataloged in Sanger database v.10.1.
Results: Unsupervised hierarchical clustering showed two major T-LL subsets separated from normal bone marrow. These subsets were not defined by any studied clinicopathological parameters. Specifically, there was an overlap in miRNA profiles when cases were classified according to the NCI-Rome criteria into high- and low-risk age and WBC groups (age groups 0 to <1 year, 1-9 years, ≥10 years; WBC groups < and ≥ $50x10^9$/L). There was no difference in miRNA expression when patients were stratified according to gender. There were 41 miRNAs differentially expressed between T-LL samples from bone marrows vs. lymph nodes. Presence of cytogenetic abnormality was a major discriminative factor for miRNA expression with alterations of chromosome 11q23 associated with highest number of differentially expressed miRNAs.
Conclusions: Our study reports miRNA expression profiles in well defined series of pediatric T-LL. Different patterns of miRNA expression are seen at different sites of involvement and cytogenetic groups of this disease. Differentially expressed miRNAs define novel groups of this neoplasm, which may aid in subclassification and class prediction.

1677 Distinct Genomic Aberrations Associated with TMPRSS2-ERG Fusion Prostate Cancer

F Demichelis, SR Setlur, R Beroukhim, S Perner, JO Korbel, C Lafargue, D Pflueger, C Pina, MD Hofer, A Sboner, MA Svensson, DS Rickman, M Meyerson, C Lee, MB Gerstein, R Kuefer, MA Rubin. Weill Cornell Medical College, New York, NY; Brigham and Women's Hospital, Boston, MA; Broad Institute of M.I.T. and Harvard, Cambridge, MA; Dana Farber Cancer Institute, Cambridge, MA; Yale University, New Haven, CT; University Hospital Ulm, Ulm, Germany.

Background: Emerging molecular and clinical data suggest that ETS fusion prostate cancer (PCA) represents a distinct molecular subclass, driven most commonly by a hormonally regulated promoter and characterized by an aggressive natural history. The study of the genomic landscape of PCA in the light of ETS fusion events is required to understand the foundation of this distinct subtype.

Design: We performed a genome-wide DNA analysis on 49 PCA samples using Affymetrix 250K SNP arrays to explore for the presence of somatic genomic alterations We also analyzed transcript data for gene fusion enrichment. We further designed a high resolution NimbleGen tiling array to look for changes in the 27 ETS family members and to map genomic breakpoints for fusion.

Results: Twenty recurrent regions were detected, mainly occurring in the form of genomic loss. Co-occurring events included losses at 9q13.32 and 1p22.1. We discovered 3 genomic events associated with ETS fusion PCA, affecting chromosome arms 6q, 7q, and 16q and in addition, demonstrated consistent transcript deregulation. 6q genomic loss in non-fusion PCA is accompanied by gene expression deregulation in an independent dataset and by protein deregulation of MYO6. In order to analyze specific copy number alterations within the ETS genes, we performed a comprehensive analysis of all 27 ETS genes and of the deleted 3Mbp genomic area between ERG and TMPRSS2 (21q) for a set of PCA samples with an unprecedented resolution of 30 base pairs. We demonstrate that high resolution tiling arrays can be used to pin-point breakpoints leading to fusion events.

Conclusions: This study provides further support to defining a distinct molecular subtype of PCA based on the presence of ETS gene rearrangements.

1678 EWS Gene Rearrangement in Epithelial Tumors

FM Deng, J Tull, CE Fuller. SUNY Upstate Medical University, Syracuse, NY.

Background: Although gene rearrangements are widely observed in a variety of hematological and soft tissue neoplasms, they have been far less frequently described in epithelial tumors. Accumulating evidence suggests that this may be due to technique issues as opposed to inherent cell specific differences between carcinomas and these other neoplasms. The EWS gene has been found to be fused with a number of different transcription factor genes in various bone and soft tissue tumors and leukemia. Recently, fusion between EWS and POU5F1 genes has been detected in a small population of hidradenoma of the skin and salivary mucoepidermoid carcinoma. The current study was undertaken to determine whether EWS gene rearrangements are detectable in other common epithelial tumors.

Design: Tissue microarrays (TMA) were constructed to contain duplicate or triplicate cores of 164 cases of numerous different carcinomas from the following sites: breast, head and neck region including thyroid and salivary gland, lung, pleura, liver, pancreas, skin, adrenal gland, and the gastrointestinal, gynecological, and urogenital systems. These TMAs were then subjected to direct fluorescence in situ hybridization using an EWSR1 break-apart probe cocktail (Vysis, Downers, Grove, IL). A positive result was reported when greater than 10% of the tumor nuclei had evidence of split red and green signals, indicative of EWS gene rearrangement.

Results: The majority of cases had virtually no nuclei with split signals, verifying an intact EWSR1 gene region in those tumors. However, 2 of 9 (22%) invasive ductal carcinomas of breast and 1 of 5 (20%) esophageal adenocarcinomas showed evidence of EWS gene rearrangement with a range of 14-22 % of tumor nuclei showing split signals. Repeated FISH on the original paraffin sections from these tumors further confirmed the positive results.

Conclusions: EWS gene rearrangements, though quite uncommon in epithelial neoplasms overall, may be rarely encountered in a subgroup of carcinomas. The current findings warrant more comprehensive testing of large cohorts of invasive ductal carcinoma of the breast and esophageal adenocarcinoma for determination of overall frequency and possible prognostic relevance of these EWS gene rearrangements, as well as for assessment of the definitive gene fusion partner(s) in these tumors.

1679 Does Androgen Receptor Have a Role in a Subgroup of ER Negative Breast Cancer?

ME Edgerton, S Sanga, E Downs-Kelley, V Cristini. UT MD Anderson Cancer Center, Houston, TX; University of Texas, Austin, TX; UT Houston Health Science Center, Houston, TX.

Background: Previously Doane et al and Farmer et al, postulated a subgroup of ER negative breast cancers that demonstrated gene expression profiles of Androgen Receptor (AR) signaling. The series were both small, with 6/22 and 10/41 patients that demonstrated the AR molecular profile in each publication. The two groups were not rigorously compared in the original reports, which were published nearly simultaneously.

Design: We combined the gene expression data from both sources, performed cross-platform normalization, and updated the probe definitions to reduce institutional bias and improve signals. We compared the presumed AR signaling subgroups across the two institutions to determine if they were equivalent, used other network inference methods to test the hypothesis that they demonstrate expression patterns that support AR signaling, and built a model to identify more patients and examine survival.

Results: We were able to build a model of presumed AR positive molecular profiles from one data source (e.g. Doane) and use it to predict the same population in the other data source (e.g. Farmer) with high accuracy. Combined data from Doane and Farmer supported AR as a signaling network that was active in that subgroup. We identified more data with presumed AR signaling from published ER negative data in the public domain that had survival data. We built a Kaplan-Meier curve for this patient population that showed poor survival; however, all of the patients for whom we could identify survival data and who expressed AR signaling network were also her-2neu positive.

Conclusions: Our results show that 1) the subgroups identified by Doane and Farmer have the same molecular profile; 2) network inference methods support a role for AR signaling in this subgroup; 3) survival data examined thus far may be biased by her-2neu status as all AR signal positive cases identified with survival data were also her-2neu positive. Doane and Farmer each reported only half of the patients with an AR signaling profile were her-2neu positive, while the other half were triple negative; however, they did not publish survival data. Previous IHC work by Ellis et al supports AR as a positive prognostic marker in the triple negative phenotype. This work supports a potential role for therapeutic intervention using AR inhibition in breast cancer.

1680 Gene Expression Alterations in Premalignant and Preinvasive Breast Disease

LA Emery, A de las Morenas, A Tripathi, P Sebastiani, CL Rosenberg. Boston University Medical Center, Boston, MA.

Background: Atypical ductal hyperplasia (ADH) and DCIS are candidate, non-obligate, breast cancer precursors based on clinical and histopathological evidence. Their relationship to invasive breast cancer remains poorly understood, as studies involving the genetic abnormalities associated with premalignant and preinvasive breast disease are limited. We aim to characterize the gene expression alteration associated with these early breast lesions.

Design: Epithelial-specific mRNA from normal-appearing breast (CN), ADH, and DCIS from 12 previously untreated surgical patients (36 lesions total) with ER+ sporadic breast cancer, were obtained by LCM of fresh frozen breast tissue. Gene expression profiles were characterized using the Affymetrix U133A array. After initial filters, Bayesian Analysis of Differential Gene Expression was used to make 3 comparisons: ADH-CN, ADH-DCIS, and DCIS-CN, with cut-off fold changes of ≥1.5. Patient-matched sets (CN-ADH-DCIS) were analyzed using a regression model with log-normal errors and a variance component per subject, taking into account that samples are matched by subjects and applying this across all genes. The data were first validated by qRT-PCR using 6 genes identified as differentially expressed: FN1, GPRC5A, CAPN6, MME, OXTR, and CDKN1C, on unamplified RNA from 8 cases used for microarray. Further validation was done on newly isolated CN, ADH, and DCIS lesions from 12 independent cases with the same 6 genes. DAVID and Ingenuity® were used for pathway analysis.

Results: We found 824 differentially expressed genes between DCIS-CN and 438 genes between ADH-CN, with 400/438 (91%) of ADH-CN genes also present in DCIS-CN. Only 61 genes were differentially expressed between ADH-DCIS. qRT-PCR validation showed all 6 genes were differentially expressed in the expected direction with 58/65 (89%) of the technical comparisons and 93/106 (88%) of the prospective comparisons validating. Biologically important pathways including focal adhesion, cell signaling, and cell cycle regulation were implicated, even in ADH-CN.

Conclusions: We conclude that ADH and DCIS epithelium from patients with sporadic breast cancer are highly similar at the gene expression level. Many of the gene expression alterations seen in DCIS have already developed by the time a histological diagnosis of ADH is reached. Pathways crucial in breast carcinogenesis are already dysregulated in the transition from CN to ADH. These data provide strong genetic evidence that ADH is a breast cancer precursor.

1681 Quantitative Proteomic Analysis of *API2-MALT1* Expression Signature by Isobaric Tags and High-Energy C-TRAP Dissociation Tandem Mass Spectrometry

SL Farmen, C Seiler, LM McAllister-Lucas, PC Lucas, KP Conlon, D Fermin, V Basrur, MS Lim, KSJ Elenitoba-Johnson. University of Michigan, Ann Arbor, MI.

Background: Quantitative proteomic analysis by mass spectrometry (MS)-based approaches permits the interrogation of complex protein mixtures. *API2-MALT1* chimeric fusion is the protein product of the t(11;18) aberration, which is the most common chromosomal alteration in extranodal marginal zone lymphoma. Despite its implication in lymphomagenesis, the signaling pathways modulated as a consequence of this chimeric fusion protein are unknown.

Design: We generated a human embryonic kidney (HEK-293) cell line that was stably transduced to express the *API2-MALT1* fusion and another that was transduced with a vector-control. Equivalent amounts of protein from each cell type were labeled using using an isobaric (iTRAQ) tag that yields amine-derivatized peptides, and subjected to MS/MS using high energy fragmentation in the C-TRAP of an LTQ-Orbitrap XL tandem mass spectrometer. The MS/MS spectra were processed using the TransProteomic Pipeline equipped with X!Tandem for protein identification. Significantly expressed proteins were determined by beta-uniform mixture modeling approach with significant differential expression defined at 0.13 false discovery rate. Identified proteins were subjected to Ingenuity pathway analysis to reveal biological pathways deregulated as a consequence of *API2-MALT1* expression, and several were validated with Western blotting.

Results: iTRAQ LC-MS/MS identified 27 proteins underexpressed (RR < 0.7) and 17 proteins overexpressed (RR >1.3) in cells overexpressing *API2-MALT1*. MALT1 was five-fold overexpressed in the experimental cells. Proteins reflective of a role for *API2-MALT1* in deregulation of apoptosis, cytokine signaling, cell cycle progression and protein transport were illuminated by pathway analysis. Among others, iTRAQ data indicated that coatomer protein gamma, SEC22b, and REM1 were overexpressed in the *API2-MALT1* positive cells, while GSPT1/eRF3, enolase, anamorsin, and serine/threonine kinase 24 were underexpressed. A subset of these were confirmed by Western blotting.

Conclusions: iTRAQ LC-MS/MS is a powerful tool for global quantitative proteomic analysis. Our studies reveal the ability of MS combined with bioinformatics-enabled discovery platforms to discover novel pathogenetic mechanisms and biomarkers that may be useful for facile identification of the disease entities.

1682 Morphometry and Object-Based Image Analysis in the Development of a Systems Pathology Based Prognostic Model for Prostate Cancer

G Fernandez, SI Fogarasi, FM Khan, M Teverovskiy, R Mesa-Tejada, MJ Donovan. Aureon Laboratories Inc., Yonkers, NY; Columbia University College of Physicians and Surgeons, New York, NY.

Background: An integrative, systems pathology platform for constructing prognostic models in prostate cancer has been developed. A key aspect has been the generation of a morphometric, object-oriented image analysis method which utilizes the Hematoxylin and Eosin (H&E)-stained specimen to extract quantitative features of tissue and cellular architecture. Using H&E sections from prostate needle biopsy (PNB) samples, we hypothesized that morphologic attributes may be important discriminators of Gleason grade and therefore associated with disease progression.

Design: Clinical-pathologic data including outcome (i.e. castrate and/ or systemic disease within 8 years of prostatectomy) and PNB specimens from 1027 patients were analyzed. A minimum of three H&E digital images were acquired and independently reviewed for tumor content, Gleason grade (GG), and quality. Using digital masking, infiltrating tumor and tumor-gland lumens were outlined. Image analysis software was used to generate quantitative histologic features based on cellular properties of the prostate cancer (e.g. tumor cells to lumen area). Domain feature association with outcome was determined by univariate Cox modeling.

Results: Twenty seven histologic features displayed significant association with disease progression in univariate analyses (c-index ≤0.4 or ≥0.6). One H&E feature that quantified tumor epithelial cells not directly associated with an intact tumor gland (univariate c-index of 0.34) was selected in a multivariate setting that included preoperative clinical data and protein biomarkers. A Kaplan-Meier curve for this feature demonstrated accurate risk stratification for disease progression in the training cohort (n=686), cut-point 0.31, p<0.00001.

Conclusions: Morphometric features extracted from H&E stained prostate cancer tissue sections—in combination with features derived from biomarker and clinical data—can significantly contribute to multivariate models in identifying patient phenotypes for outcome-based risk stratification. This study further suggests that an objective, quantitative evaluation of GG can be approached with object-based image analysis algorithms.

1683 IKBKe Copy Number Gain in Lung Adenocarcinoma

R Firestein, JA Barletta, A Ligon, M Loda, WC Hahn, LR Chirieac. Brigham and Women's Hospital, Boston, MA; Dana Farber Harvard Cancer Center, Boston, MA.

Background: Molecular alterations in non-small cell lung cancer are investigated to define new prognostic markers and therapeutic targets. IKKe, encoded by the gene IKBKe, is a protein that activates nuclear factor kappa B (NF-kB). IKBKe was recently identified as a possible oncogene amplified in breast cancer with potential therapeutic implications. Although IKBKe is amplified in lung cancer cell lines, the amplification and expression status in lung adenocarcinoma is unknown.

Design: We studied 87 consecutive patients with lung adenocarcinomas treated with surgery at Brigham and Women's Hospital. Histopathologic characteristics were recorded and IKBKe copy number alterations assessed by fluorescence in situ hybridization (FISH) recorded as no gain, gain, gain with polysomy, and polysomy. IKKe expression by immunohistochemistry was assigned to one of four categories: no staining (score=0); minimal staining (score=1); intermediate staining (score=2); strong staining (score=3). We evaluated clinicopathologic predictors of IKBKe copy number alterations and IKKe expression and associations with survival.

Results: IKKe copy number alterations were present in 45 carcinomas (71%). IKKe expression levels were significantly higher in lung adenocarcinomas than in adjacent normal parenchyma (p<0.0001) and correlated with gene copy number gain (p=0.04). The IKKe expression score in lung adenocarcinomas was 0 in 16 (17.8%) cases, 1 in 28 (31.1%) cases, 2 in 31 (34.4%) cases, and 3 in 15 (16.7%) cases. Lung carcinomas with high IKBKe expression correlated with lymph node metastases (p<0.0001).

Conclusions: Our study showed that a significant number of lung adenocarcinomas have IKBKe copy number gains and increased IKKe expression by immunohistochemistry. IKKe expression levels correlated with gene copy number gain and lymph node metastases. Our findings suggest that IKKe may serve as a potential therapeutic target for a subset of patients with lung adenocarcinoma.

1684 Interrogation of WNT Signaling Pathway Activation in Adrenocortical Carcinoma by Transcriptome Profiling

TJ Giordano, R Kuick, DG Thomas, T Else, M Vinco, D Sanders, G Hammer. University of Michigan, Ann Arbor, MI.

Background: WNT signaling pathway activation is a hallmark of colon cancer and common to many tumors types, including those of the adrenal cortex.

Design: To assess the relative significance of WNT activation in adrenocortical carcinoma (ACC), we combined genome-wide gene expression profiles derived from DNA microarray analysis of a large cohort of tumors with molecular markers of WNT activation. Specifically, we annotated the ACCs by β-catenin immunohistochemistry and CTNNB1 mutational analysis.

Results: Using this approach, we identified, using p<0.01 and fold change >1.5 as selection criteria, a list of 811 unique differentially expressed genes in ACC related to WNT pathway activation. Bioinformatic evaluation of these genes revealed an overrepresentation of genes related to cell adhesion, the WNT signaling pathway, and genes with LEF1 promoter binding sites. Kaplan-Meier survival analysis revealed that ACCs with WNT pathway activation were associated with a slightly poorer outcome.

Conclusions: Collectively, these results indicate that WNT signaling pathway activation is a biologically significant event in approximately one-third of ACCs, a finding with pathogenetic and therapeutic implications.

1685 Genes Are Differentially Expressed in Normal-Appearing Breast Epithelium between Cohorts of Breast Cancer Cases When Compared to Reduction Mammoplasty Controls

K Graham, A Tripathi, A de las Morenas, P Sebastiani, C Rosenberg. Boston University Medical Center (BUMC), Boston, MA.

Background: Genetic abnormalities have been identified in preinvasive breast lesions. The normal-appearing epithelium (NlEpi) from breast cancer patients (cancer normal, CN) is not well-characterized, but may also contain genetic abnormalities. We have shown that gene expression of NlEpi from reduction mammoplasty controls (RM) differs from NlEpi from ER+ breast cancer cases (CNER+). Here we compare the NlEpi from RM controls to NlEpi from a population of immunophenotypically heterogeneous untreated breast cancer patients. We expanded the RM-CNER+ comparison by adding new cases and extended our study by comparing RM controls to NlEpi from ER- breast cancer cases (CNER-). We also conducted a more robust statistical analysis and performed tight age matching between cases and controls.

Design: 63 fresh frozen breast tissues were collected from BUMC's Pathology Department; 10um sections were prepared and NlEpi was microdissected. RNA was extracted, amplified and hybridized to an Affy U133A chip. Data were preprocessed with Affy GCOS 1.4 software. Data analysis was performed with Bayesian Analysis of Differential Gene Expression with subsequent 80% extrinsic cross-validation of gene lists. Microarray results were technically validated with qPCR using unamplified RNA from the original cases. 7 test (ATF3, BTG2, CLU, EGR1, FOS, IER2, NR4A2) and one control primer (CPSF6) were used. Gene lists were analyzed with DAVID and Ingenuity Pathways Analysis (IPA).

Results:

Comparison	RM-CN	RM-CNER+	RM-CNER-
# samples	18 RM, 18 CN (9 CNER+, 9 CNER-)	17 RM, 17 CNER+	10 RM, 10 CNER-
# probes (genes)	90 (88)	84 (80)	194 (186)
Technical Validation % (# validated/total)	88 (35/40)	93 (28/30)	90 (28/31)
Pathway Analysis (top 3 canonical pathways from IPA)	-ERK/MAPK Signaling -IL-10 Signaling -Neurotrophin/ TRK Signaling	-RAR Activation -Oxidative Stress -Gene Reg. by Peroxisome Proliferators via PPARα	-Hypoxia-Inducible Factor Signaling -FXR/RXR Activation -LXR/RXR Activation

Prospective qPCR validation of NlEpi RNA from a set of 36 independent age-matched RMs and CNs is ongoing.

Conclusions: Gene expression differs among the NlEpi of women without breast cancer and age-matched women with ER+ or with ER- breast cancer. Pathways that may participate in early breast cancer progression are deregulated even before the cells are phenotypically abnormal.

1686 Homogenate Based Assays for Apoptosis May Cause a Misleading Result

D He, J Slisz, J Johnson, C Miller, B Firestone, L Zawel, J Li, M Caprio, R Mosher. Novartis Institutes for Biomedical Research, Inc., Camdridge.

Background: Detection of apoptosis can be used as a pharmacodynamic marker to evaluate the anti-tumor effect. These studies can be performed on tumor homogenates or histological analysis. The purpose of this study was to evaluate both methods that might impact the readout of our studies.

Design: Colo 205 and A2058-derived xenograft tumors were treated with compounds known to induce apoptosis. Xenograft collected both formalin fixed for IHC/histology and frozen for homogenate preparation. Cleaved Caspase 3 IHC was scored using the Aperio Image analysis system. The anti-human CAIX antibody was performed to define hypoxic regions. In parallel, Caspase 3 enzymatic activity was measured in homogenates using the both TruPoint Caspase-3 Assay and Caspase-Glo 3/7 Assay.

Results: Histologic examination revealed the fast growing A2058 tumors to be very heterogeneous in both the vehicle and treated animals. CC3 activation was observed around necrotic areas in both vehicle and treated tumor. Necrotic areas co-localized with CAIX antibody expression suggest that hypoxia may cause activation of CC3. Manual exclusion of necrotic areas of IHC slides allowed differences between treated and non-treated groups to be observed. Following normalization to the vehicle group the CC3 induction attributed to drug treatment was approximately14 fold. Interestingly, the homogenate assay failed to discern this difference. In contrast to the A2058 tumors, slow growing Colo 205 xenograft tumors were well defined with few necrotic areas. Caspase 3 profiling was performed in Colo205 tumors following treatment with the DR5 antibody. The CC3 IHC and CC3 enzymatic homogeneous assay gave concordant results in this non-necrotic xenograft.

Conclusions: It is necessary to understand tumor growth behavior and tissue composition prior to choosing a homogenate or slide based assay.

1687 Germline Stem Cell Protein Piwil2-Deficiency Alters Tumor Spectrum in p53-Deficient Mice

G He, QT Yan, L Chen, Y Ye, RL Shen, SH Barsky, HF Lin, JX Gao. Ohio State University, Columbus, OH; Yale University School of Medicine, New Haven, CT.

Background: Piwil2 (alias mili in mouse) is a member of Ago/Piwi family of proteins containing Piwi and PAZ domains (PPD). The PPD proteins participate in RNA interference (RNAi) at transcriptional and posttranscriptional levels. Recently, we have found that piwil2 is stably expressed in pCSCs and regulates their proliferation in vitro,

suggesting that piwil2 plays an important role for tumor development. Therefore, we investigated whether piwil2-decificiency effects tumor development.
Design: Since p53-deficienct mice spontaneously develop tumors with lymphoma being dominant, we crossed $p53^{-/-}$ mice with $mili^{-/-}$ mice to generate $p53^{-/-}mili^{-/-}$, $p53^{-/-}mili^{+/-}$, and $p53^{-/-}mili^{+/+}$ mice. The tumor incidence was monitored and the tumor spectrum was examined by histopathology. To investigate the mechanisms underlying the tumor type changes, precancerous stem cells (pCSCs) were established from lymphoma or sarcoma and transplanted subcutaneously into Scid mice.
Results: Most mice (~80%) with $p53^{-/-}$ phenotype were male [80% of $p53^{-/-}milli^{-/-}$ mice (12/15), 78.5% of $p53^{-/-}mili^{+/-}$ mice (11/14) and 100% $p53^{-/-}mili^{+/+}$ mice (3/3)]. All $p53^{-/-}mili^{-/-}$, $p53^{-/-}mili^{+/-}$, and $p53^{-/-}mili^{+/+}$ mice developed tumors. In $p53^{-/-}milli^{-/-}$ mice, 80% of the mice developed high grade malignant fibrohistiocytoma-like spindle cell sarcoma and high grade angiosarcoma (12/15), and only 20% of the mice developed lymphoma (3/15). In contrast, 64.28% of $p53^{-/-}milli^{+/-}$ mice developed sarcoma and angiosarcoma (9/14), and 38.7% of them developed lymphoma or leukemia (5/14). $P53^{-/-}milli^{+/+}$ mice were dominant with lymphoma (2/2). The lifespan between $p53^{-/-}mili^{-/-}$, $p53^{-/-}mili^{+/-}$ and $p53^{-/-}mili^{+/+}$ mice was not statistically significantly different, although $p53^{-/-}mili^{-/-}$ mice appeared to die earlier than $p53^{-/-}mili^{+/-}$ and $p53^{-/-}mili^{+/+}$ mice. Interestingly, stromal pCSC lines were established from lymphoma with $p53^{-/-}mili^{-/-}$ or $p53^{-/-}mili^{+/-}$ genotypes, and vice versa. The stromal pCSCs could develop both high grade lymphoma and sarcoma after transplanted into Scid mice.
Conclusions: Our studies demonstrate that Piwil2-deficiency may alter tumor spectrum in $p53^{-/-}$ mice in a gene dose-dependent manner and implicate that lymphoma and sarcoma may originate from the same pCSCs. The outcomes of pCSCs reconstituting tumors may be affected by environmental cues.

1688 S-Adenosylhomocysteine Hydrolase Downregulation Contributes to Tumorogenesis

J Hernandez-Losa, M Lleonart, A Carnero, R Somoza, S Ramon y Cajal. Hospital University Vall d Hebron, Barcelona, Spain; Spanish National Cancer Research Center (CNIO), Madrid, Spain; Madrid, Spain.
Background: With an aim to discover novel genes involved in cell proliferation, a genome-wide loss-of-function genetic screen was performed to identify additional putative tumor suppressor genes. To date, five genes have been identified from differing biochemical families. In this project, one of these genes was focused on, namely S-Adenosylhomocysteine hydrolase (SAHH), and its role in human tumors.
Design: The SAHH gene function was characterized in MEFs. The expression of SAHH was overexpress with cDNA and downregulart with siRNA. Cell proliferation was analyzed by the Crystal Violet method, and β -galactosidase activity was performed to identify the senescent cells. In human tumors, the level of expression of SAHH was studied in a cancer profiling array with 206 samples of varying tumors using real-time PCR. We corroborate the results in a set of 40 patients with colorectal tumors by real-time PCR and Western-Blot. Both the normal and tumoral samples of each patient were evaluated.β
Results: The in-vitro results show that SAHH inactivation confers resistance to both p53 and p16INK4-induced proliferation arrest. Interestingly, SAHH inactivation inhibits p53 transcriptional activity and impairs DNA damage-induced transcription of p21Cip1. Moreover, SAHH downregulation modulates senescence in primary cells. In human tumors SAHH mRNA was lost in 50% of tumor tissues tested, including up to 15 different types in comparison to normal tissue counterparts. Moreover, SAHH protein was also affected in some colon cancers.
Conclusions: With these results we propose that SAHH a gen related with the turnover of adenosine, and homocysteine is downregulated in a large number of tumors and may represent an important novel tumor-supresor gene.

1689 A Paradigm for Biomarker Discovery Combining Expression Array Data Mining and Tissue-Based Validation

MD Hofer, S Kageyama, T Tanaka, K Nakagawa, T Hori, LR Chirieac, J Fukuoka. Brigham and Women's Hospital, Boston, MA; Toyama University Hospital, Toyama, Japan.
Background: Lots of published expression array data is available on the internet but not often utilized. We describe the in silico analysis of expression data and validation of dysregulated genes on a multi-tumor tissue microarray.
Design: Expression data was mined using the internet-based platform Oncomine for genes dysregulated in cancers that are routinely and experimentally evaluated and had limited reports on PubMed. Dysregulation was validated in 1150 patient samples of 14 tumor types with IHC on a 4-tier system and correlated with clinical (chi-square test) and outcome data (Kaplan-Meier analysis).
Results: Of 65 genes initially, Calgranulin B (mac387), Lamin B, and CD138 met all of our selection criteria. Expression varied in tumor types.

Mean Staining Intensities

	Calgranulin B	Lamin B	CD138
pulmonary SCC (PSCC)	1.1	1.1	1.6
pulmonary adeno ca (ADC)	0.5	1.0	0.7
breast ca	0.2	1.1	0.8
RCC	0.1	1.0	0.4
bile duct ca	0.2	1.0	0.8
thyroid ca	0.0	1.0	0.8
HCC	0.1	0.9	1.6
colon adeno ca (CADC)	0.2	1.2	1.1
gastric ca	0.1	1.1	0.7
prostate ca (PrCA)	0.0	0.5	0.2
pancreatic ca (PaCA)	0.1	1.0	0.4
urothelial ca	0.5	1.5	1.5
ovarian ca (OCA)	0.2	1.0	0.5
endometrial ca (ECA)	0.3	1.2	0.5

Calgranulin B expression was significantly associated with stage in ECA, lymph node metastases (LNM) in OCA, lymphovascular invasion (LVI) in PSCC (all $p<0.05$) and survival in CADC (log-rank p=0.0261, mean follow up 34 mo). CD138 expression was significantly associated with LVI in PADC, stage in PSCC, stage and LNM in PrCA (all $p<0.05$) and survival in PADC (log-rank p=0.001, mean follow up: 54 mo) and CADC (log-rank p=0.006). Lamin B expression was significantly associated with stage in PaCA, and stage, LVI, and LMN in PADC (all $p<0.05$) in which it was also associated with survival (log-rank p=0.003).
Conclusions: We demonstrate the use of internet-based gene expression analysis of published data and validation in tissue samples as approach to facilitate biomarker discovery. Using established and novel IHC markers, we found associations with tumor progression and survival for several tumors. We believe that pathologists are in a unique position to validate previously reported dysregulated genes in patient tissue thus allowing for streamlined biomarker discovery.

1690 Virtual-Karyotyping with SNP Arrays Is a Useful Approach for the Diagnosis of Morphologically Difficult Renal Cell Neoplasms

HJ Kim, SS Shen, LD Truong, JY Ro, AG Ayala, K Alvarez, Z Gatalica, J Bridge, FA Monzon. The Methodist Hospital Research Institute, Houston, TX; Inje University College of Medicine, Sanggye Paik Hospital, Seoul, Korea; Creighton University, Omaha, NE; University of Nebraska, Omaha, NE.
Background: Renal epithelial neoplasms are morphologically and clinically heterogeneous and have characteristic chromosomal imbalances that can be used for classification. Even after ancillary testing, approximately 7% of tumors remain uncategorized [renal cell carcinoma (RCC) unclassified], limiting optimal patient management. In this study, we applied virtual-karyotyping derived from SNP microarrays (v-karyotype) to a cohort of morphologically difficult renal epithelial neoplasms to determine if this approach can assist in achieving a specific histopathologic classification.
Design: Twenty-six morphologically difficult cases defined as cases in which seven genitourinary surgical pathologists could not achieve a consensus diagnosis were subjected to v-karyotyping using the Affymetrix GeneChip 10K 2.0 or 250K Nsp mapping arrays. Subsequently, the v-karyotype data obtained was reviewed to determine if it could be diagnostically informative.
Results: Five cases were removed due to 100% concordance among pathologists and 3 cases failed to yield adequate v-karyotypes. Eighteen cases with no consensus diagnosis (13) or a consensus diagnosis of RCC unclassified (5) were selected for final analysis. From the "no consensus" cases, 8 cases reached a majority-vote diagnosis and 5 cases did not. All cases without a majority-vote diagnosis or with a diagnosis of RCC unclassified were able to be classified based on the presence of characteristic chromosomal abnormalities (e.g. loss of 3p for clear cell RCC). Virtual karyotypes confirmed the majority-vote diagnosis in 6 of 8 cases (3 clear cell with -3p, 2 papillary with +7/+17 and 1 chromophobe with loss of multiple chromosomes); two cases showed disagreement with the majority-vote: 1 case with papillary morphology and loss of 3p on the v-karyotype and one oncocytoma in which the v-karyotype was not characteristic of any reported subtype.
Conclusions: Our results show that morphologically difficult renal neoplasms can be classified based on the chromosomal imbalances detected by virtual-karyotyping with SNP arrays. Virtual karyotyping is a useful approach for the diagnosis of renal tumors, including cases diagnosed as RCC unclassified and yields classification information that can be used to determine optimal patient management.

1691 Automated Quantitative Proteomic Analysis Platform (HISTORX): Clinical Application and Comparison with Routine Immunohistochmeistry among Diffuse Large B-Cell Lymphoma (DLBCL) Patients (Pts)

A Klimowicz, N Bahlis, A Magliocco, D Demetrick, L Difrancesco, D Stewart, A Mansoor. Tom Baker Cancer Ctr., Calgary, AB, Canada; University of Calgary/CLS, Calgary, AB, Canada.
Background: DLBCL is a heterogeneous & aggressive disease with unpredictable clinical course. Biological markers like GCB vs. ACB phenotype; bcl2 / p53 has been evaluated by immunoperoxidase (IPOX) staining; but with inconclusive results. Quantifying protein expression (Ki-67; p53; ER/PR), by IPOX is "observer" dependent and semi-quantitative. The AQUA automated quantitative pathology system (HISTORX) is proteomic analysis platform. It quantitates absolute number of protein molecules within discrete sub cellular locations by combining fluorescence-based image analysis with automated microscopy. This pilot study evaluated the clinical applicability of HistoRX in comparison with routine IPOX by correlating these scores with Overall survival in DLBCL pts.
Design: Triplicate (0.6-mm) cores from FFPE tissue at diagnosis (2001-04) were used for tissue microarray (TMA). TMA sections were stained with CD20, CD3 & Ki-67 antibodies using standard protocol (Ventana -AZ). Visual estimation of IPOX staining was recorded in 10% increments (>50% was considered as high Ki-67). TMA sections stained with anti-Ki-67 (MIB1-Dako1:200) were used for Fluorescent immunohistochemistry. Automated image acquisition was performed by the HistoRx PM-2000™ and analyzed by AQUA® script. Mean AQUA scores (nuclear compartment) separated pts into the binomial variables of high (>50%) and low positive, using hierarchical clustering analysis (Ward's method). Fisher's exact test, Kaplan-Meier / Mann-Whitney non-parametric tests were used for statistical analysis.
Results: 56 pts (35M/21F); median age 66 yrs (range 34-86) were included. 21/56 (38%) had stage I/II and (62%) had stage III/IV. Pts were treated with CHOP (41%) or RCHOP (59%) regimens; median follow-up was 22M. By HistoRX, OS was favorable among pts with high Ki-67 (86% vs. 67%; p = 0.056) . High Ki67 has significant predictive

value among CHOP group (88% vs. 46%; p = 0.034) compared to RCHOP (88% vs. 86%; p = 0.737). High Ki-67 staining by IPOX did not show any association with OS in all (79% vs.75%, p = 0.928) or among pts treated with CHOP (58% vs. 63%, p = 0.518) or RCHOP (88% vs. 82; p = 0.320).
Conclusions: HISTORX provides superior quantification of proteins in tissues compared to routine IPOX and further studies are required to evaluate clinical applicability of this novel technique.

1692 Deregulation of MicroRNA Expression in Metastatic Breast Cancer – *"of Mice and Women"*

M Lacroix-Triki, G Maillot, S Beck, L Roger, P Zindy, T Filleron, H Roche, S Vagner. Institute Claudius Regaud, Toulouse, France.
Background: miRNAs are short noncoding RNAs which trigger translational down-regulation or increased degradation of the target mRNA. If recent studies have shown altered miRNA expression in cancer, few ones explore the role of miRNAs in the metastatic process. Using high-throughput technologies, we have studied miRNAs expression in a mouse model of metastatic mammary cancer, and in a series of breast cancers.
Design: The mouse model consisted of orthotopic injection of 4 mammary cancer cell lines, giving rise to tumors with different metastatic potential. 67NR tumors showed no metastasis, 168FARN and 4T0 tumors had intermediate invasive potential, whereas 4T1 tumors led to lung metastasis. Thirty mice were injected, tumors were harvested and total RNA extracted. High-throughput miRNAs profiling was performed using microarray in collaboration with the EMBL facility (V. Benes). Expression of selected miRNAs was validated by northern blot and quantitative RT-PCR. In addition to miR-10b, we focused on 3 miRNAs highly expressed in the metastatic tumors 4T1, and studied their expression in 34 metastatic and non-metastatic breast cancers, using RT-qPCR. miRNAs expression was correlated to clinico-pathological data, with special regards to the distant metastatic outcome.
Results: Microarray analysis of the 30 mouse tumors allowed identification of a set of 47 miRNAs that could accurately classify each tumor.

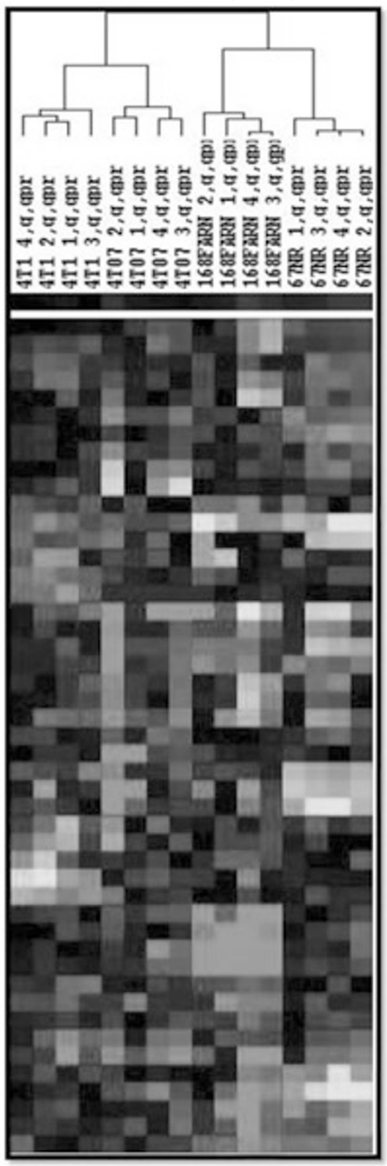

Each tumor type was characterized by a specific cluster of over-expressed miRNAs, which was cross-validated by northern blot and RT-qPCR analysis. Among the 4 selected miRNAs that were highly expressed in the metastatic tumor 4T1, one showed a significant association to metastatic outcome in our series of 34 invasive breast cancers.
Conclusions: In a translational study from a metastatic mouse model to human tumors, we could identify miRNAs with altered expression in metastatic breast cancer, thus providing new insights in the complex deregulation of gene expression leading to metastatic progression.

1693 Global Gene Coexpression Analysis Identifies a Poor Prognosis Signature across Tumor Types

AC Ladd, CI Dumur, CN Powers, DS Wilkinson, CT Garrett. Virginia Commonwealth University, Richmond, VA.
Background: Global gene expression data are currently being used in attempts to develop cancer survival prediction tools. A predictor with power across tumor types has utility especially for use with uncommon cancers for which gene expression data sets are small and therefore molecular characterization is incomplete. Standard biostatistical methods build predictors from comparisons between two or more phenotypic classes while a novel approach, utilized here, focuses on identifying sets of genes coexpressed across all samples.
Design: Microarray gene expression data (Affymetrix GeneChips®) from 136 tumors from 15 sites of origin were used to calculate coexpression measures. Two biologically relevant modules of highly coexpressed genes (mitosis and immune response), were detected in our data set. A "coexpression signature" comprised of the 186 genes in the two modules was tested for survival prediction against the entire set of tumors. Using Cox proportional hazard regression analysis methods (with gene expression measures as variables), a prognostic index was computed for each case which was then used to assign it to a high or low risk group. Leave-One-Out-Cross-Validation methods were used to ensure unbiased risk group assignment. Kaplan-Meier (KM) survival curves were then generated for each group.

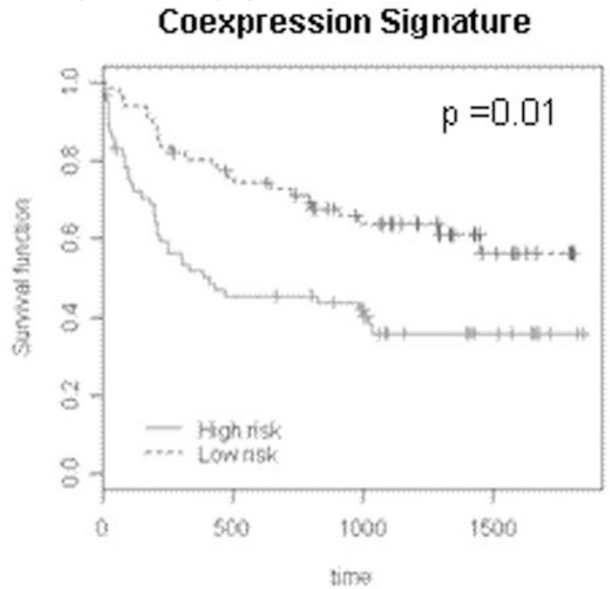

Results: Risk prediction based on these methods was statistically significant (p=0.01). Interestingly, there was a high level of agreement between the genes in the coexpression signature and two other signatures based on undifferentiated tumors (one developed from our data set and another previously published by Chinnaiyan et al, PNAS, 2004), although KM curves generated from these signatures showed no significant differences between the two groups (p=0.12 and p=0.18, respectively).
Conclusions: While mitosis and immune response are not novel pathways to be uncovered in cancer, the coexpression analysis performed here refined the large list of genes in these pathways to those most likely contributing to their disruption. Therefore, not only are these types of methods of potential use in cancer risk assessment, but they may be useful in identifying new targets for therapeutic intervention.

1694 Micro RNA Profile of High Grade Prostate Carcinoma

KRM Leite, JM Sousa-Canavez, ST Reis, LH Camara-Lopes, M Srougi. University of Sao Paulo Medical School, Sao Paulo, Brazil; Genoa Biotechnology, Sao Paulo, Brazil.
Background: Although incidental prostate cancer (PCa) has been reported in up to 80% of autopsies, only a small percentage of men will die from the disease. There is a biological continuum from an indolent tumor to a highly aggressive and potentially fatal form. Treatment options are variable from active monitoring to palliative androgen-ablation. PSA, Gleason score and clinical stage are the main prognostic factors, but there is an urgent need for new molecular markers to be applied in the identification of unfavorable disease. MicroRNAs (miRNAs) are small (20–22 nucleotides) regulatory RNAs that complementary binding to mRNA sequences repress target-gene expression. A large number of miRNAs has been related to the development of neoplasias, and are denominated oncomirs. The aim of our study is to determine a profile of miRNA related to high grade PCa that could be used as prognostic marker for therapeutic decisions.

Design: Nineteen patients underwent radical prostatectomy for treatment of localized high grade PCa. The mean age was 64.4 years old, mean Gleason score 8.6, and mean tumor volume 11.6 cc. Eighteen were staged pT3N0 and one pT3N1. Fourteen miRNA were studied by quantitative real time PCR. The specimens of six retropubic prostatectomies for treatment of benign prostate hyperplasia were used as control. The endogen control was β2-microglobulin.

Results: The results are in figure 1. The majority of miRNA was shown to be overexpressed. mi-218, mi-let7 and mi-100 were overexpressed in 18 from 19 cases (94.7%) and mi-25 was overexpressed in 17 from 19 (89.5%). mi-Let7 has been called as a tumor suppressor miRNA since it regulates negatively the expression of Ras and c-Myc, the later related to PCa aggressiveness. But conversely we found it overexpressed by almost 95% of our cases.

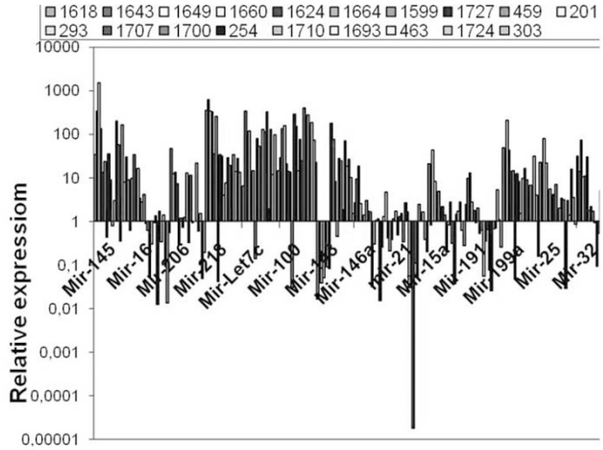

Conclusions: Each miRNA has around 100 genes targets, and their expression is tissue specific. The meaning of specific profiles of miRNA in human tumors is only beginning to be understanding and more studies with large series have to be conducted in order to turn this information useful in the clinical practice.

1695 Suppression of Glucosylceramide Synthase Gene Expression: A Novel Approach for Cancer Treatment

Y-Y Liu, GA Patwardhan, D Ying, M Jazwinski, J Bao. University of Louisiana, Monroe, LA; Tulane University School of Medicine, New Orleans, LA; Lousiana State University Healthe Science Center, Shreveport, LA.

Background: Glucosylceramide synthase (GCS) is pivotal enzyme in ceramide metabolism and ceramide induced-apoptosis pathway. This enzyme catalyzes the transfer of ceramide into glucosylceramide, a key step in glycosphingolipid biosynthesis and is associated with reduced signaling of apoptosis. GCS has recently been implicated in the cytotoxic response of cancer cells to chemotherapy. Our previous works and those of others indicated that GCS confers drug resistance via defecting ceramide induced-apoptosis pathway by disrupting drug uptake in cancer cells. This study evaluates the effects of GCS expression on reversal of drug resistance.

Design: Antisense oligonucleotides were synthesized to target human GCS gene expression. The expression and knockdown of GCS gene were assessed by quantitative PCR, Western blot and ceramide glycosylation assay. The influences of antisense oligonucleotides on GCS expression and on chemosensitivity were examined in drug-resistant cell lines (MCF-7-AdrR, and EMT6/AR1) and in tumor-bearing mice. The effects of overexpression GCS gene, cell response to chemotherapy agent and treatment sensitivity were evaluated in these animal models. Microarray analysis of chemo-sensitized gene expression was performed using Affymetrix Human Genome U133 Plus 2.0.

Results: Suppression of GCS overexpression by treatment of antisense oligonucleotide sensitized all drug-resistant cancer cell lines to doxorubicin *in vitro*. Knockdown GCS by antisense gene transfection significantly inhibited tumor growth from the inoculation of drug-resistant cancer cells (MCF-7-AdrR) *in vivo.*

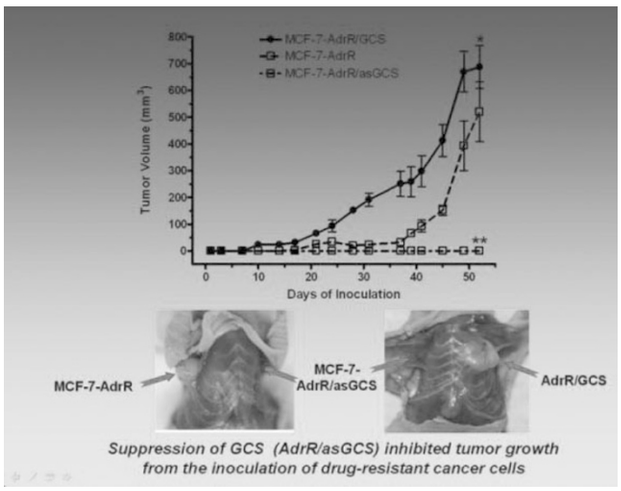

The treatment of antisense oligonucleotide (mixed backbone, methyl-RNA-DNA) suppressed tumor growth to 30% as compared with scrambled control groups and sensitized doxorubicin efficacy by 3-fold in orthotopic breast tumor models.

Conclusions: The present study demonstrated glucosylceramide synthase (GCS) is a potential novel target for drug-resistance reversal and suppressing the overexpression of GCS might be an effective approach to improve cancer chemotherapy.

1696 Atypical 11q Deletions Identified by Array CGH May Be Missed by FISH Panels for Prognostic Markers in Chronic Lymphocytic Leukemia

MC Mammarappallil, SR Gunn, MK Hibbard, M Lowery-Nordberg, EL Enriquez, ME Gorre, MS Mohammed, RS Robetorye. The University of Texas Health Science Center at San Antonio, San Antonio, TX; Clarient Diagnostics Laboratory, Aliso Viejo, CA; Louisiana State University Health Sciences Center, Shreveport, LA; Combimatrix Molecular Diagnostics, Irvine, CA.

Background: Genomic alterations have increasingly gained importance as prognostic markers in chronic lymphocytic leukemia (CLL). The identification of genetic alterations of prognostic importance in CLL is currently accomplished using commercially available FISH panels that can detect the most common recurrent aberrations involving chromosomes 11q, 13q, 14q, 17p and whole chromosome 12. Although the use of FISH analysis has improved the detection rate of genomic alterations in CLL from approximately 50% using conventional cytogenetics to more than 80%, there is a need for improved methods to identify prognostic markers that can aid in the risk-stratification of these patients. Recently, array comparative genomic hybridization (array CGH) has been gaining acceptance as a diagnostic tool that can also be applied to detect genomic gains and losses of prognostic importance in CLL.

Design: Bacterial artificial chromosome array-based array GCH was used to detect recurrent genomic alterations in 190 cases of CLL using a clinically validated array designed to interrogate all known CLL prognostic loci.

Results: This analysis identified 22 CLL cases with 11q deletions, with 20 cases that included the *ATM* gene in the deleted region. However, three of the CLL cases showed atypical 11q deletions, with one case exhibiting a centromeric breakpoint just proximal to the *ATM* locus, and two cases exhibiting proximal breakpoints telomeric to the *ATM* gene. FISH analysis using an LSI ATM probe failed to detect the 11q deletions in all three CLL cases.

Conclusions: In the current study, we present three CLL cases with atypical 11q deletions that were not properly identified by a commercially available five probe FISH panel that included an 11q22 LSI ATM probe. This study is the first to report CLL cases with large 11q deletions that did not include the *ATM* gene, suggesting that additional genes in this region may be important for the pathogenesis of CLL. Although FISH analysis has contributed tremendously to the molecular cytogenetic understanding of the CLL genome, it is clear that many important genomic aberrations may be missed by currently available FISH prognostic marker panels.

1697 Aberrant Co-Expression of D2-40 and CD31/CD34 in Vascular Neoplasm Is an Indicator of Aggressive Behavior

T Maruno, T Tanaka, MD Hofer, Y Iinuma, K Nakagawa, T Hori, J Fukuoka. Toyama University Hospital, Toyama, Japan; Brigham and Women's Hospital, Boston.

Background: Recent recognition of lymphatic vascular markers has unveiled biological events in the formation of lymphatic and blood vessel network. Yet, their expression in various vascular tumors are not carefully observed. Understanding the expression profiles and interactions of those markers in vascular tumor is important which may lead to a better understanding of lymphangiogenesis and angiogenesis in various diseases.

Design: A Tissue microarray was constructed from 40 hemangioma, 8 lymphangioma, 13 pyogenic granuloma, 3 endothelioma, and 4 angiosarcoma cases with duplicated cores. We analyzed the expression of D2-40, CD31 and CD34 with immunohistochemistry using consecutive TMA slides. Staining results were scanned by a virtual slide system (VS-100, Olympus), and the expression compared among the slides.

Results: Cells with positive D2-40 staining were observed in 55% of hemangioma, 100% of lymphangioma, 38% of pyogenic granuloma, 67% of endothelioma, and 100% of angiosarcoma. The neoplastic vessels with CD34 expression were found in all except two lymphangioma cases and one hemangioma case. Remarkable co-expression of D2-40 & CD31 was frequently found in lymphangioma (38%(3/8)), endothelioma;

(33% (1/3)), and angiosarcoma (100% (4/4)), and rarely in hemangioma (5% (2/40) and pyogenic granuloma (7.2% (1/13)). Similarly, high co-expression of D2-40 and CD34 was also found in the same tumors. Especially, three out of four cases of angiosarcoma and two out of three cases of endothelioma showed relatively diffuse and strong co-expression in D2-40 and CD31.

	Expression(%/positive cases)			Coexpression(%/positive cases)	
Disease(N)	D2-40	CD31	CD34	D2-40&CD31	D2-40&CD34
Hemangioma(40)	55%/22	100%/40	98%/39	5%/2	2.5%/1
Lymphangioma(8)	100%/8	85%/7	75%/6	38%/3	50%/4
Pyogenic granuloma(13)	38%/5	100%/12	100%/12	0%/0	7.2%/1
Endothelioma(3)	67%/2	67%/2	100%/3	33%/1	67%/2
Angiosarcoma(4)	100%/4	100%/4	100%/4	100%/4	50%/2

Conclusions: Our results indicate that the aberrant co-expression of D2-40/CD31 or D2-40/CD34 are a common event in lymphangioma, endothelioma, and angiosarcoma. In the tumor of blood vessel, excluding lymphatic vessels, aberrant expression can be an indicator of aggressive nature, and may also be useful diagnostic marker.

1698 A Gene Expression Profile of Non-Neoplastic Colonic Sigmoid Epithelium

WD Mojica, L Stein, J Luce, LA Hawthorn. Univ @ Buffalo, Buffalo, NY; RPCI, Buffalo, NY; Medical College of Georgia, Augusta, GA.

Background: A rational approach to biomarker discovery involves the identification of differentially expressed genes between diseased and non-diseased cells of the same lineage. This is particularly true for colon cancer which demonstrates a molecular step-wise progression from normal to cancer. To date, an expression profile completely representative of non-neoplastic colonic epithelial cells (NNCEC) has not been reported. Because of an inability to maintain NNCEC in culture, expression profiles have come from various sources. These results may be biased due to several factors: tissue sections because of cellular heterogeneity; FFPE material from degradation; and colon cancer cell lines thought to be differentiating to NNCEC due to growth in an artificial environment and genotypic drift. Herein is presented the expression profile data from unfixed, enriched NNCEC with high molecular integrity run on an high density expression array.

Design: NNCEC were procured by exfoliation and enrichment from 10 separate patients undergoing segmental resection of the sigmoid for diverticular disease. E*x vivo* bias was minimized by keeping the time between extirpation and placement of cells into buffer under 10 minutes. A highly enriched population of NNCEC was obtained through the dissolution of mucus, lysis of rbc's and the use of immunomagnetic beads. Extracted RNA was run on the Human Exon 1.0 ST Array to evaluate whole transcript and alternative splicing events. Principal component analysis (PCA) was performed on the NNCEC data and compared to colorectal cancer (CRC) data. Differentially expressed genes were identified through the comparison with publicly available CRC expression data.

Results: There were 4302 alternative splicing events in the exon array data. The NNCEC samples were distincly segregated from the CRC data by PCA. A total of 3828 differentially expressed genes were identified between the NNCEC and the publicly available colon cancer data with 2505 genes upregulated and 321 downregulated in the CRC data relative to the NNCEC.

Conclusions: A baseline of knowledge is needed before any comparative analysis can be performed. The absence of such a baseline may lead to errant conclusions particularly if the sample assayed possesed an inherent bias. The rapid acquisition of unfixed, enriched cells means a reproducible baseline expression profile can be established for NNCEC, the proverbial starting point from which to assess pathology in the sigmoid colon.

1699 A Bioinformatic Approach to Identify New Metabolic Targets in Prostate Cancer

C Priolo, J Lamb, G Zadra, D Oldridge, E Palescandolo, E Sicinska, M Loda. Dana Farber Cancer Institute, Harvard Medical School, Boston, MA; Brigham and Women's Hospital, Harvard Medical School, Boston, MA; Broad Institute, Harvard and MIT, Cambridge, MA.

Background: Cancer cells undergo fundamental changes in their metabolism, including a shift from mitochondrial respiration to a higher rate of glycolysis and an increase in *de novo* fatty acid synthesis. To this end, we focused our attention on the role of the metabolic enzyme Fatty Acid Synthase (FASN) as an oncogene and a potential drug target in prostate cancer (PCa), and showed that FASN overexpression is able to transform immortalized prostate epithelial cells (PrECs).

Design: We used gene microarray data and KEGG as pathway visualization tool to map metabolic changes induced by FASN during transformation of PrECs. In order to identify drugs that could contrast these metabolic effects, we applied the bioinformatic approach "Connectivity Map", which uses pattern-matching tools to detect similarities between gene expression signatures of cells treated with various drugs and those obtained by overexpressing or silencing genes. We compared the transcriptome of PrEC-FASN to gene expression data from human cancer cells treated with an extensive library of compounds.

Results: FASN-driven transformation of PrECs is characterized by a remarkable increase in the expression of enzymes of glycolysis and oxidative phosphorylation, in addition to the expected lipid synthesis boost. These results suggest a global impact of FASN overexpression on the metabolism of normal as well as cancer cells. By the Connectivity Map approach, we obtained a list of 14 drugs inducing gene expression profile changes that were inversely correlated with the FASN signature, thus being potentially able to inhibit the FASN phenotype. Some of these compounds are known metabolic poisons, while others are currently in the clinic for non-tumor applications, though they were not previously known for their properties as metabolic perturbagens.

Conclusions: We mapped metabolic changes induced by FASN in prostate epithelium and identified compounds potentially able to neutralize the FASN metabolic phenotype. Pre-clinical validation of these compounds is ongoing.

1700 Lung Adenocarcinoma and Its Stroma: Tissue Proteomics Reveals Differential and Compartment-Specific Roles for the Homologs Transgelin and Transgelin-2

MH Roehrl, JH Rho, JY Wang. Massachusetts General Hospital, Boston, MA; Brigham and Women's Hospital, Boston, MA.

Background: Early detection of lung adenocarcinoma progression and discovery of underlying functional mechanisms are hampered by a large dynamic concentration range of tissue biomacromolecules and the fact that current proteomic approaches are limited by the presence of relatively few highly abundant proteins.

Design: To overcome this limitation, we first developed heparin affinity chromatography enrichment (HAFE) as a powerful technique to significantly enrich for low-abundance components. HAFE-enriched protein extracts from five fresh-frozen paired normal and adenocarcinoma tissues were then studied by 2-D difference gel electrophoresis (DIGE) and tandem mass spectrometry (MS/MS). Additional independent paired tissue samples were studied by Western blotting, immunohistochemistry, and RT-PCR.

Results: Fourteen proteins were found differentially expressed in neoplastic versus normal tissue. The identities of three protein spots were elucidated by tandem mass spectrometric (MS/MS) sequencing as transgelin (TAGLN), transgelin-2 (TAGLN2), and cyclophilin A (PPIA). All three proteins were overexpressed in lung adenocarcinoma tissue. The protein expression levels were further validated by Western blotting of both unfractionated total protein and HAFE-enriched extracts from 15 paired lung adenocarcinoma samples. Four paired lung squamous cell carcinoma and 9 paired colon adenocarcinoma samples were also studied as controls. Semi-quantitative RT-PCR indicated that both TAGLN2 and PPIA are upregulated at transcriptional level. Intriguingly, we found by immunohistochemistry that the overexpression of TAGLN was strictly localized to the tumor-induced reactive stromal tissue compartment, while the overexpression of TAGLN2 was exclusively localized to the neoplastic glandular compartment.

Conclusions: We discovered that two homologous proteins, TAGLN and TAGLN2, which possess 87% amino acid sequence similarity, display striking mutually exclusive and complementary spatial and cell type expression regulation (*i.e.*, tumor stroma *vs.* neoplastic epithelial cells). Our work describes the discovery of novel candidate biomarkers of lung adenocarcinoma that may advance basic pathophysiologic understanding of lung adenocarcinoma, as well as early diagnosis, treatment guidance, and treatment response monitoring.

1701 MicroRNA-based Assay for Diagnosing Tumor Tissue Origin

S Rosenwald, I Barshak, D Lebanony, H Gibory, L Cohen, Y Goren, I Leizerman, D Nonaka, A Tobar, Z Bentwich, R Aharonov, N Rosenfeld, D Cohen. Rosetta Genomics, Rehovot, Israel; Sheba Medical Center, Tel-Hashomer, Israel; Tel-Aviv University, Tel-Aviv, Israel.

Background: Cancer of unknown primary (CUP) constitutes 3%~5% of all newly diagnosed cancer cases. It presents a major diagnostic challenge due to the therapeutic implications of the tissue origin of the cancer. MicroRNAs are a family of non-coding, regulatory RNA genes that are involved in oncogenesis and show remarkable tissue-specificity. In previous work we demonstrated that using a set of only 48 microRNAs with a biologically-motivated classification procedure, tissue of origin could be identified with high accuracy. Here we develop this potential of microRNA into a practical diagnostic assay.

Design: Hundreds of primary and metastatic tumor FFPE samples were collected. High-quality RNA, including the well-preserved microRNA fraction, was extracted from the FFPE blocks using proprietary protocols. Expression levels of potential microRNA biomarkers were profiled using a sensitive and specific qRT-PCR platform. Advanced classification algorithms were developed to utilize the information of the microRNA expression patterns for the diagnosis of tumor origin.

Results: Using expression levels of a panel of microRNAs in qRT-PCR, tissue of origin could be accurately identified and a diagnostic assay based on this technology was defined. The performance of the assay was validated using an independent test set.

Conclusions: Previous studies have highlighted the tissue-specificity of microRNA expression, and have demonstrated the potential of microRNA expression for accurate identification of tumor tissue of origin. Here we developed this potential into a diagnostic assay, based on a qRT-PCR platform. This assay produces reproducible, accurate results, and provides an important new tool for diagnosing tumor tissue origin.

1702 MALDI Imaging of Tissue Microarrays – Mass Spectrometry Identification of Tumor Proteome

A Seager, J Melamed, A Kogos, T Remsen, S Formenti, P Pevsner. NYU SOM, NY, NY.

Background: Mass spectrometry of tissue microarrays (TMA) can characterize the proteome of multiple cancers. MALDI Imaging of tumors has been reported previously by the authors.*1-3* Tentative protein identifications can be obtained with MALDI Imaging. We hypothesized that a TMA could provide specific protein characterization of tissue.

Design: Five µm sections were obtained from a TMA composed of thirteen cores: prostate cancer (5), normal prostate (7), and control liver tissue (1), figure 1. Contiguous sections were obtained for MALDI imaging and H&E stain. Sinapic acid matrix for MALDI imaging was applied by sublimation. MALDI images were exported to BioMap, and the mass of the prominent proteins identified. Tentative protein indentifications were displayed as orange color on the MALDI images.

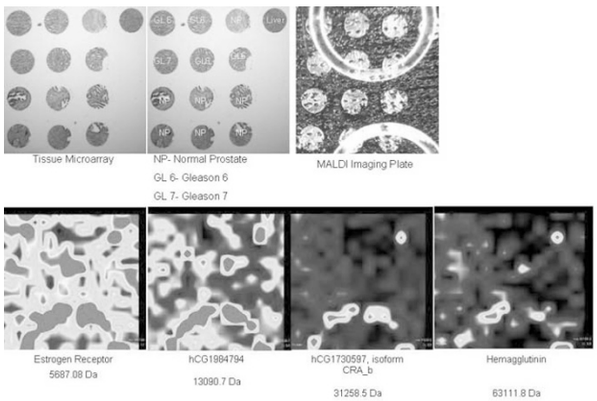

MALDI imaging of proteins can separate normal from tumor tissue. Estrogen receptor and hCG2984794 expressed in normal and tumor. hCG1730597 and hemagglutinin only expressed in normal tissue.

Figure 1

Results: All proteins were present in liver tissue. The proteins in tumor and normal tissue were estrogen receptor 13090.7 Da, hCG1984794 14884.1 Da, and immunoglobulin mu heavy chain16005.4 Da. The following proteins were only identified in normal tissue: L1 protein [Human papillomavirus type 6] 16679.7 Da,ORF1 protein[Hepatitis E virus]31258.5 Da,hCG1730597,isoform CRA_b 61541.8 Da, Solute carrier family17, member7 61541.8 Da, and hemagglutinin[Influenza B virus (B/Delaware/04/2007)] 63111.8 Da.

Conclusions: MALDI imaging can be used to identify proteins from a TMA. The expressed proteins can separate tumor from normal tissue. Further studies should allow increased resolution of MALDI images, and higher correlation with Gleason grade in prostate and malignancy grade in other tumors. 1. Pevsner PH, Melamed J, Remsen T, et al. Mass Spectrometry MALDI Imaging of Colon Cancer Biomarkers- A New Diagnostic Paradigm. Biomarkers in Medicine 2008 in Press;. 2. Pevsner P, Formenti S, Remsen T, et al. Mass Spectrometry of Buccal Mucosa. Biomarkers for Biodosimetry in Radiation Incidents 2008. Bethesda, MD 3. Pevsner PH, Naftolin F, Hillman DE, et al. Direct identification of proteins from T47D cells and murine brain tissue by matrix-assisted laser desorption/ionization post-source decay/collision-induced dissociation. Rapid Commun Mass Spectrom 2007;21:429-36.

1703 Characterization of Long-Surviving Glioblastomas by High Resolution Array Comparative Genomic Hybridization (aCGH)

S Sharma, A Free, Y Mei, SC Peiper, Z Wang. Medical College of Georgia, Augusta, GA.

Background: Glioblastoma is the most common primary brain tumor with a median survival of about 12 months, despite multimodal treatment. Nevertheless, a small fraction of glioblastoma patients have long-term survival; very little genomic data is available to explain this long survival. Aiming to identify genes critical to evolution of this favorable subset, we performed high resolution aCGH in long-surviving glioblastomas.

Design: Following receipt of Human Assurance Committee approval, three cases of long surviving glioblastomas (over 24 months) with age range 55 to 62 years were identified at our institution. Two of these were histologically usual glioblastoma, and one a gliosarcoma variant. Paired biopsies at initial diagnosis and recurrence (24 months) were examined in one case. Two others had only one biopsy with optimal tissue for analysis (one at initial diagnosis and other at recurrence). Representative sections from formalin-fixed, paraffin-embedded (FFPE) tumor tissues showing optimal histology were utilized for DNA extraction using the TrimGen Wax Free kit and analyzed for DNA copy number changes using Affymetrix SNP250K chips.

Results: DNA from archival FFPE tissues yielded adequate coverage, as assessed by analysis of SNPs. Initial biopsies had no chromosomal or subchromosomal gains or losses. The case with paired samples illustrated that recurrent tumor had accumulation of significant chromosomal losses and gains, with limited overlap (chromosome 10). One case had amplification of EGFR gene in initial specimen. The gliosarcoma had amplification of WNT5B. There were no detectable abnormalities in the P53 pathway. Abnormalities in the PI3K pathway were limited to PTEN loss. One patient had a hemizygous deletion of PTEN at initial diagnosis and its loss of heterozygosity in the recurrence, which also had deletion of P16. There were no other abnormalities of genes in the RB1 pathway. All three cases had a deletion in chromosome 20q of approximately 140kb that contained 4 genes (one with a family member expressed in neurons and mutated in Charcoat-Marie-Tooth disease).

Conclusions: Glioblastomas with prolonged survival present with limited abnormalities in gene copy number. Relatively few copy number changes involved families of genes known to play key role in regulation of tumor growth. Array CGH analysis of GBM should provide informative molecular karyotypes. Larger future studies with unbiased, genome-wide profiling carry the potential to identify genomic insight into clinical subgroups of GBM.

1704 Biomarkers of Rb Signaling Loss Are Characteristic of High Grade Adnexal Serous Carcinoma

PA Shaw, A Chun, A Milea, A Tone, H Begley, J Greenaway. University Health Network, Toronto, ON, Canada.

Background: Overexpression of p16, a tumor suppressor gene, is frequent in ovarian cancer, and as a response to cellular stress in a cell with intact p16/Rb signaling, will result in proliferation arrest. A compromised Rb pathway however will lead to increased p16 expression and continued proliferation. This study proposes to determine the differential expression of p16/Rb pathway genes in ovarian cancer, as assessed by expression profiling and protein expression by immunohistochemistry, and to determine if alterations in the p16/Rb pathway predict for histologic type and clinical outcome.

Design: All carcinomas, tissues, and tissue microarrays were identified and retrieved through the UHN Biobank. Differential gene expression of p16, cyclin D1, Rb, cyclin E, and E2F transcription activators in high grade serous carcinomas (HGSC) and normal tubal epithelium (FTE) was determined after profiling microdissected normal tubal epithelium and 13 high grade serous carcinomas using Affymetrix U133 Plus 2.0 arrays. Immunohistochemistry for p16, cyclin D1, and MIB1 was performed using standard techniques. Stained tissue microarray sections, representing 468 ovarian tumors, were digitally scanned, and protein expression scored according to percentage tumor cells positive and staining intensity, with their sum determining the final histoscore. Fisher's exact test with 95% confidence intervals was used to determine the significance of results.

Results: Expression profiles revealed significantly increased expression of p16, E2F1, E2F3, and cyclin E genes in HGSC compared to normal FTE ($p<0.05$). Cyclin D1 was down regulated in cancers, and there was no significant change in Rb1 gene expression. By IHC, p16 was overexpressed in both serous (80%) and non-serous carcinomas (36%), but a high p16/high MIB1 signature was significantly more common in HGSC than in non-serous cancers ($p=0.003$).

Conclusions: High grade serous carcinoma has increased p16 expression, and expression profiles indicate this is often associated with decreased cyclin D1, increased cyclin E, and increased E2F transcription activators, reflecting compromised Rb signaling, and allowing cells to bypass senescence and increase proliferation. Preliminary protein expression data suggest that overexpression of p16 in a nonfunctional Rb pathway may be a potential biomarker of HGSC.

1705 A New Type of Antibody-Mediated Rejection of Kidney Transplants Defined by Endothelial Changes

B Sis, GS Jhangri, S Bunnag, B Kaplan, PF Halloran. University of Alberta, Edmonton, Canada; University of Illinois, Chicago.

Background: HLA antibody is a risk factor for kidney transplant loss due to antibody-mediated rejection (ABMR) but is not specific for ABMR. C4d staining of peritubular capillaries in biopsies is specific for ABMR but insensitive. We hypothesized that, in biopsies from patients with HLA alloantibody, altered expression of endothelial genes would detect ABMR negative for C4d.

Design: We identified 119 endothelial cell-associated transcripts (ENDATs) from the literature. We studied 173 consecutive renal allograft biopsies for cause, using microarrays to examine the relationship of ENDAT expression to HLA antibody, pathology, and survival.

Results: Mean ENDAT expression was increased in C4d positive ABMR and correlated with pathologic lesions and HLA antibodies. Many individual ENDATs were increased in C4d positive ABMR vs. T cell-mediated rejection, and correlated with increased graft failure, particularly von Willebrand's factor (VWF). In patients with HLA antibodies, ENDATs identified C4d negative biopsies that resembled C4d positive ABMR, with transplant glomerulopathy, increased scarring, and increased graft loss, although with less inflammation. C4d positive and C4d negative ABMR accounted for most of the graft losses (14/17).

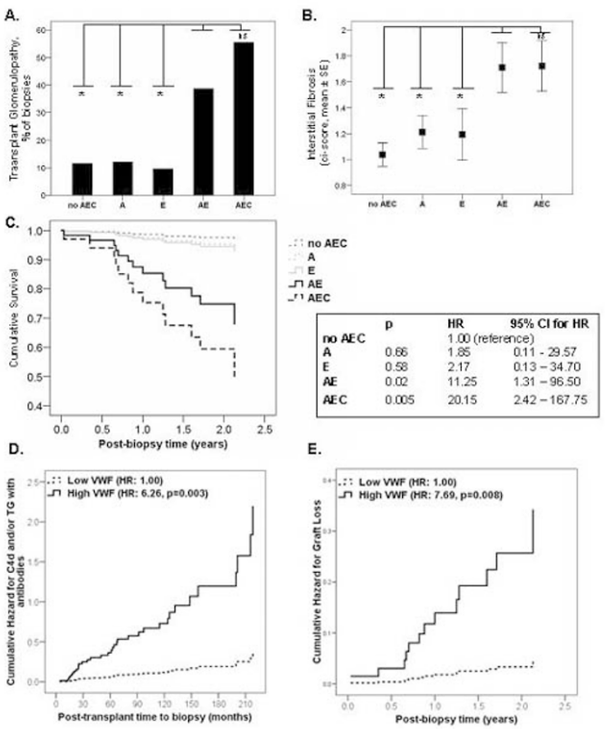

	p	HR	95% CI for HR
no AEC		1.00 (reference)	
A	0.66	1.85	0.11 - 29.57
E	0.58	2.17	0.13 – 34.70
AE	0.02	11.25	1.31 – 96.50
AEC	0.005	20.15	2.42 – 167.75

Figure 1. Graft pathology and survival in biopsies grouped according to the presence of Ab (A), C4d (C), and increased VWF expression (E).

Conclusions: In biopsies from patients with HLA antibodies, increased expression of endothelial transcripts was associated with features of ABMR and subsequent graft loss (sensitivity 91% and 79%, respectively) whether C4d was positive or negative. Compared with C4d, endothelial transcripts in biopsies represent a sensitive approach for detecting kidney transplants at risk for alloantibody-mediated deterioration.

1706 Mass Spectrometry Based Proteomic Analysis of AL Amyloidosis: Immunoglobulin Light Chain Gene Constant Region Is an Invariable Part of Amyloid Deposits and Provides Valuable Diagnostic Target

JD Theis, JA Vrana, JD Gamez, A Dogan. Mayo Clinic, Rochester, MN.

Background: AL Amyloidosis, caused by immunoglobulin light chain (LC) deposition, is a well-recognized complication of plasma cell neoplasms. So far no pan-proteomic analysis of AL amyloidosis has been performed and the real constituents of AL amyloid is not known. To understand the constituents of AL amyloidosis, we undertook a comprehensive study of AL amyloidosis using a novel mass spectrometry (MS) based proteomic approach.

Design: Paraffin embedded tissue from 100 cases of AL amyloidosis was studied. Amyloid deposits were microdissected, processed and trypsin digested into peptides. The peptides were analyzed by nano-flow liquid chromatography electrospray tandem MS. The resulting MS data were correlated to theoretical fragmentation patterns of tryptic peptide sequences from the Swissprot database using Scaffold algorithm. The identified proteins were subsequently examined for the presence or absence of amyloid related peptides.

Results: MS gave peptide profiles consistent with AL amyloidosis in each case. The analysis showed λ-LC deposition in 66 and κ-LC in 34 cases. In each case, MS confirmed the previous clinicopathological diagnosis. Peptides representing LC constant region were always present. The average coverage of the λ-LC and κ-LC constant regions were 40% and 55%, respectively. Additionally, the distribution of the peptides suggested that in most cases whole of the LC constant region was deposited. MS also identified λ-LC variable region peptides in 37 of 66 cases and κ-LC variable (V) region peptides in 29 of 34 cases studied. The V region coverage was more restricted and the peptides identified were frequently within the framework segments. It is likely that the peptides derived from CDR segments were present but not detected by the methodology due to somatic hypermutation. In the cases with the LC V region hits, it was also possible to assign V region family usage. λ-LC cases frequently used V region I, II and III families whereas, in κ-LC cases, V region I and III families dominated.

Conclusions: 1) AL amyloidosis can be accurately diagnosed MS based proteomic analysis in routine clinical specimens. 2) AL amyloidosis invariably contains LC constant region peptides and, frequently, the whole of the constant region is deposited. 3) It is possible to identify LC V region family usage using MS based proteomic analysis. In the clinical setting, this information may be helpful in predicting organ distribution and clinical outcome.

1707 Multiplex Quantum Dot ISH in Tissue Microarrays Identifies HOXA9 and DNMT3A as Unfavourable Markers in Acute Myeloid Leukaemia

E Tholouli, S McDermott, JA Hoyland, C Glennie, R Swindell, JA Liu Yin, RJ Byers. Manchester Royal Infirmary, Manchester, United Kingdom; University of Manchester, Manchester, United Kingdom; Christie Hospital, Manchester, United Kingdom.

Background: Validation of prognostic genes identified by microarray expression profiling is required in clinical samples. We have developed a quantum dot (QD) based multiplexed *in-situ* hybridization (ISH) method for quantitative localization of mRNA targets in formalin fixed paraffin embedded tissue (FFPET) which we used to identify prognostic genes in AML.

Design: Fifteen tissue microarrays (TMAs) were made using FFPET bone marrow trephine samples from 240 patients with AML treated at Manchester Royal Infirmary with standard chemotherapy between 1994 and 2005, of which 192 patients were suitable for analysis. Samples were represented in triplicate and a whole blood white cell pellet used as standard. QD-ISH was performed for nine candidate prognostic genes in AML using triplex QD-ISH for: Bcl2, survivin and XIAP; DNMT1, DNMT3A and DNMT3B; HOXA4, HOXA9 and Meis1. Signal intensity was measured by spectral imaging and scrambled oligonucleotides used to measure background staining. Background noise was corrected for by dividing expression of anti-sense probes by that of scrambled probe followed by normalization of expression values against the standard. Statistical analysis was performed using chi-square and Mann Whitney-U tests and overall survival (OS) and disease free survival (DFS) used in Kaplan-Meier analysis.

Results: Median age was 52 years and the OS was 43% at 5 years with 80% complete remission (CR) after induction. Low expression of HOXA4 was associated with improved OS ($p=0.013$) and DFS ($p=0.025$) on univariate and multivariate analysis. High expression of HOXA9 ($p<0.0001$) and DNMT3A ($p=0.04$) were associated with failure to achieve CR. High expression of Meis1 was of borderline significance for poor response to chemotherapy ($p=0.05$). The other 5 genes showed no correlation with CR, DFS or OS.

Conclusions: These results demonstrate the utility of a novel standardized, quantitative multiplex QD-ISH method for identification of prognostic markers in FFPET. The advantages of the method are its application to TMAs, enabling high throughput, use of archived materials and transferability across a spectrum of malignancies.

1708 RUNX1T1: A Novel Putative Progression Marker in Pancreatic Endocrine Neoplasms: An Immunohistochemical Analysis

LM Turner, E Henderson, J Helm, M Ghayouri, NA Nasir, BA Centeno, SV Nicosia, L Kvols, A Nasir. University of South Florida, Tampa, FL; Moffitt Cancer Center and Research Institute, Tampa, FL.

Background: Clinical outcome of pancreatic endocrine neoplasms (PENs) is difficult to predict based on morphology alone. Using complimentary microarray data analytic tools, we discovered a novel set of putative progression genes (PPGs) that were differentially expressed in metastatic primary pancreatic endocrine carcinomas (MP-PECAs) relative to non-metastatic primary pancreatic endocrine tumors (NMP-PETs) and validated a newly discovered PPG using IHC.

Design: PENs resected at our institution were evaluated for size, histologic grade, angioinvasion, perineural invasion, lymph node and liver metastases. Cases were grouped as MP-PECAs or NM-PETs based on the presence or absence of metastases at the time of resection of the pancreatic primary. To determine RUNX1T1 expression in NMP-PETs and MP-PECAs, we performed IHC using TMA on 24 PENs. IHC was also performed on matched histologically normal pancreatic islets. An IHC score, called an H score, was calculated to represent the amount of protein expression in each case by multiplying the percentage of cells staining (used as a whole number) by the intensity of the stain (1 least, 3 most).

Results: Cases with multiple metastases showed the most profound loss of expression of RUNX1T1 with a mean H score of 36.67 versus 127.38 for NMP-PETs. In cases with liver metastases at the time of surgery, the H score was 47.57 compared to 127.38 for NMP-PETs. Of note, 90% of MP-PECAs had low H scores (below 80), while 79% of NMP-PETs had high H scores (above 80), and this difference was statistically significant ($p=.003$). Lastly, comparing the histologically normal pancreatic islet cells in cases with metastases with those without metastases shows an average of 56.67% of islet cells staining positive in cases with MP-PECAs versus 79.67% in NMP-PETs.

Conclusions: RUNX1T1 appears to be a novel marker of metstatic potential in low-grade PENs. The presence of liver metastases at the time of surgery is closely associated with low expression levels of RUNX1T1 in primary pancreatic endocrine tumors compared to cases without metastases, and this was statistically significant ($p = 0.003$). Our results suggest that decreased RUNX1T1 expression by IHC could be used as a surrogate marker for the presence or absence of liver metastases, validating its role as a prognostic indicator.

1709 microRNA Regulation of *VHL* Gene in Clear Cell Renal Cell Carcinomas

VA Valera, BA Walter, WM Linehan, ME Sobel, MJ Merino. National Cancer Institute, Bethesda, MD; American Society of Investigative Pathology, Bethesda, MD.

Background: Loss of expression of the tumor suppressor gene *VHL* is a well known mechanism in the pathogenesis of hereditary and sporadic Renal Cell carcinomas (RCCs). In the disease, *VHL* silencing has been found to be mediated by either mutations or gene promoter methylation. However, the role of microRNA expression on *VHL* inactivation and therefore their influence on the onset and progression of RCCs has not been investigated yet. Therefore, the aim of this study was to evaluate the role of microRNAs on *VHL* gene inactivation and its correlation with clinicopathogic features in clear cell RCCs.

Design: Database search identified two microRNAs as potential regulators of the *VHL* gene by base pair complementarity: Hs-miR-320 and hs-miR-92. These two microRNAs and the target gene were analyzed by real-time PCR in a series of clear cell RCC and their corresponding paired normal tissue from FFPE tissue sections. A two-fold change (Up or down) in the Tumor-to Normal ratio (T/N) was determined as significant. MicroRNA expression was also correlated to the clinicopathologic features of the tumors. The relationship between these variables was evaluated by the Mann-Whitney or Kruskall-Wallis non-parametric tests and significance was defined as $p<0.05$.

Results: Ten cases of clear cell RCC were analyzed. Ninety percent of the tumors showed increased expression of miRNA-320 compared to the corresponding normal tissue with a median increase of the Tumor-to-Normal expression ratio of 5.35 fold. The pattern of expression for miRNA-92 was more heterogeneous with only 40% of the tumors showing overexpression. High expression of miRNA-320 correlated consistently ($p<0.05$) with a decreased expression of VHL gene protein and mRNA, and higher expression levels were found in cases with a higher Fuhrman nuclear grade (Median miRNA-320 T/N ratio= 4.35 in Fuhrman III cases vs.3.93 in Fuhrman II; $p=0.670$) and in female patients (5.57 vs. 1.83; $p=0.05$).

Conclusions: This is the first report of microRNA regulation of the *VHL* gene in kidney cancer, where overexpression of miRNA-320 appeared as an additional mechanism involved in VHL mRNA gene regulation in clear cell RCCs. Since hsa-miR-320 is also predicted to regulate other key factors in the VHL pathway, the reuslts have a great impact on disease diagnostics, monitoring and therapy.

1710 Immunohistochemistry Enhances Proteomic Profiling from Paraffin-Embedded Tissue Sections by Mass-Spectrometry: A Novel Approach with Wide-Ranging Potential Applications in Pathology

JA Vrana, JD Gamez, JD Theis, A Dogan. Mayo Clinic, Rochester, MN.

Background: We have recently shown that the proteome of amyloid extracellular deposits can be reproducibly identified in paraffin-embedded tissue sections with great sensitivity and specificity using nano-flow liquid chromatography electrospray tandem mass spectrometry (LC-MS/MS) based proteomic analysis (Lab Invest, 2008 Aug 18 Epub). In this study, we illustrate the principle of utilizing immunohistochemistry (IHC) to successfully identify differentially expressed proteins in 2 physiological subsets of skeletal muscle.

Design: Tissue sections of normal skeletal muscle were stained with a monoclonal antibody (MY32) to fast skeletal muscle myosin. Individual muscle cells that stained positive and negative were laser microdissected and collected into separate tubes. The dissected cells were processed and trypsin digested into peptides. The peptides were analyzed by LC-MS/MS, and the resulting data were correlated to theoretical fragmentation patterns of tryptic peptide sequences from the Swissprot database using Scaffold. Peptide identifications were accepted if they could be established at greater than 90.0% probability and protein identifications were accepted if they could be established at greater than 90.0% probability and contain at least 2 identified spectra. The identified proteins were subsequently examined for the presence or absence of

muscle related peptides.
Results: LC-MS/MS gave peptide profiles containing 60 proteins consistent with a variety of fast and slow twitch muscle proteins as well as numerous general muscle protein markers. 12 of 37 proteins identified by IHC were specific to fast twitch muscle (most abundant proteins being beta-enolase and fast skeletal myosin light chain 2) and 6 of 26 proteins identified by negative IHC were specific to slow twitch muscle (most abundant proteins being myosin light chain 3 and myosin regulatory light chain 2). General muscle markers, such as myoglobin, were observed in both stained and unstained cells.
Conclusions: Our study shows that detailed proteomic analysis can be successfully performed on IHC stained tissue sections. Using this methodology, the proteome of single muscle cells can be identified and subtle differences in protein expression between physiological subsets of skeletal muscle can be demonstrated. As this technology is readily applicable to routine clinical biopsy specimens, it is likely that LC MS/MS-based proteomic analysis will have wide ranging applications in biomarker discovery and clinical diagnosis.

1711 Phosphoscan Analysis of Mantle Cell Lymphoma Cell Lines

A Zamo, TL Gu, RD Polakiewicz, A Parisi, A Bertolaso, S Barbi, G Inghirami, F Menestrina. University of Verona, Verona, Italy; Cell Signaling Technology, Inc., Danvers, MA; University of Torino, Turin, Italy.
Background: Mantle cell lymphoma (MCL) constitutes about 5% of non-Hodgkin lymphoma in the western world. It shows a characteristic clinical behaviour with initial response to therapy followed by relapses and death in 3-5 years. Many studies have investigated MCL pathogenesis by high-throughput techniques such as gene expression profiling, but very few have attempted the study of MCL from a proteomic point of view. In our previous work, we have focused our attention on the phospho-proteome of several MCL cell lines by IMAC pre-fractionation and 2D-PAGE/MS.
Design: In this work we used the PhosphoScan approach, which has already been successfully used in the phospho-profiling of lung cancer and acute myeloid leukemia. This involves a protein extraction followed by a digestion. Phosphorylated peptides are then immunoprecipitated by anti-phosphotyrosine antibody followed by capillary electrophoresis and MS identification of eluted peptides. We analysed four MCL cell lines (MAVER-1, Jeko-1, Rec-1 and Granta-519).
Results: 421 unique peptides were identified, corresponding to 341 proteins. Of these, 191 were present in at least two cell lines, and were further analysed for KEGG pathway. This analysis showed that the most represented ones are "Regulation of actin cytoskeleton" (16 proteins, 9.04%), "Focal adhesion" (15 proteins, 8.47%), "Fc epsilon RI signaling pathway" (14 proteins, 7.91%) and "B cell receptor signaling pathway" (13 proteins, 7.34%). The four pathways are strongly interconnected, and suggest the activation of the B-cell receptor in these cell lines. The absence of the antigen during in vitro culture suggests that these cell have a tonic BCR signalling either by abnormalities of the signalling pathway or by self-stimulation.
Conclusions: The BCR signalling pathway is promising from a therapeutic point of view, and recent data indicate that it might be very important in the pathogenesis of DLBCL. Its importance in MCL has not been investigated so far. PhosphoScan analysis of MCL cell lines suggests that tonic BCR signalling might be one of the mechanisms driving cell survival and proliferation in MCL, but these data need to be validated by functional studies and by the extensive analysis of tissue samples.

1712 TMPRSS2 Gene Rearrangement in Non-Prostatic Epithelial Tumors

C Zanardi, J Tull, S Zhang, C Fuller. SUNY Upstate Medical University, Syracuse, NY.
Background: Transmembrane serine protease 2 (TMPRSS2) is an androgen-regulated member of the type two transmembrane protease family (TTSP) that is normally expressed to a variable degree in prostate, colon, stomach, liver, testicle, kidney and pancreas. The TMPRSS2 (21q22.3) gene has been recently observed to be fused with several of the ETS-transcription factor family members, including ERG (21q22.2), ETV1 (7q21.2) or ETV4 (17q21), in a significant percentage of prostate carcinomas. The current study was undertaken to determine whether TMPRSS2 gene rearrangements are detectable in other common non-prostatic epithelial tumors.
Design: Tissue microarrays (TMA) were constructed to contain duplicate or triplicate cores of 164 cases of a variety of carcinomas from the following sites: breast, head and neck region including thyroid and salivary gland, lung, pleura, liver, pancreas, skin, adrenal gland, and gastrointestinal, gynecological, and urogenital systems. These TMAs were then subjected to direct fluorescence in situ hybridization (FISH) using a bacterial artificial chromosome (BAC)-derived TMPRSS2 gene dual-color break-apart probe cocktail. A positive result was reported when greater than 10% of the tumor nuclei had evidence of split red and green signals, indicative of TMPRSS2 gene rearrangement. A parallel analysis of TMAs containing prostate carcinomas was used for comparison.
Results: All tested non-prostatic epithelial tumor cases showed very rare or no tumor cell nuclei with split FISH signals, confirming an intact TMPRSS2 gene region in these tumors. In contradistinction, 62% of tested prostate carcinomas harbored demonstrable TMPRSS2 gene rearrangements.
Conclusions: These findings demonstrate absence of TMPRSS2 gene rearrangements in an extensive sampling of non-prostatic epithelial tumors, supporting the concept that TMPRSS2 alterations are unique and specific to carcinomas of prostatic origin. More comprehensive screening of similar large cohorts of epithelial tumors will be necessary to determine the incidence of rearrangements of ETS family members involving alternate fusion partner genes or other novel gene rearrangements in non-prostatic epithelial tumors.

1713 The Use of Itraq and Mass Spectrometry To Study Multiple Myeloma Associated with Bortezomib Resistance

JH Zhao, J Chen, K Evans, H Chang. University Health Network and University of Toronto, Toronto, Canada.
Background: Bortezomib, a novel proteasome inhibitor, represents a promising new clinical strategy presently deployed in clinical trials of relapsed and refractory multiple myeloma (MM). However, only 30-40% of MM patients respond to this treatment. The mechanism of resistance is not understood. Our previous study on the molecular cytogenetic profiles of MM showed that the response to bortezomib in MM patients is independent of high-risk genomic aberrations. In order to gain insights into the mechanisms of bortezomib resistance, we examined the proteome of bortezomib sensitive and resistant MM cells by comparative global proteomic analysis.
Design: Two myeloma cell lines, 8226/S (bortezomib senbsitive) and 8226/R5 (bortezomib resistance) were used in this study to determine differentially expressed proteins possibly directly involved in the acquisition of bortezomib resistance. The proteins of bortezomib sensitive and resistant cells were simultaneously identified and quantified by using isobaric tag peptide labeling (iTRAQ) technology, followed by hybrid quadruple time-of-flight mass spectrometry (MS). The MS based multiple-reaction-monitoring (MRM) technique was used to independently verify the quantitative differences of the protein expression levels between the two cell lines.
Results: The iTRAQ labeling combined with MS approach identified a large population of 665 proteins from MM cells. Among those proteins, 176 proteins (27%) were found differentially expressed between 8226/S and 8226/R5. Of the 176 proteins, 115 (65%) were up-regulated whereas 61 (35%) were down-regulated. These proteins can be classified into several major cellular pathways involving cell proliferation, differentiation, nuclear acid metabolism, molecular transport and protein synthesis. Several selected highly expressed proteins such as DEN1C, Ubiqulin-4, SCFD1 may be considered as potential protein biomarkers for bortezomib resistance.
Conclusions: iTRAQ in concert with MS is a powerful approach to identify differentially expressed proteins related to drug resistance in MM. Further verification and functional analysis of the proteins of interest in MM bortezomib resistance are ongoing.

Techniques

1714 Dermatopathology in the Digital Era

A Al Habeeb, D Ghazarian. UHN, Toronto, ON, Canada; Timmins Hospital, Timmins, ON, Canada.
Background: Teledermatopathology has the potential to deliver quality service to underserviced areas. Our airms are: To validate teledermatopathology as a diagnostic tool in underserviced areas To test its utilization in inflammatory and melanocytic lesions To compare the impact of 20x and 40x resolution on diagnostic accuracy.
Design: A total of 103 cases were studied. Routine skin cases (n=79) from Timmins were scanned at 20x using aperio 5 slides scanscope. A pathologist diagnosed these cases using light microscopy. Subsequently, these were provided to a UHN pathologist along with the information on the requisition . The pathologist was blinded to the diagnoses. Additional 12 cases of inflammatory skin biopsies (IS)and 12 melanocytic lesions (ML) were scanned at 20x and 40x with an emphasis on assessing objective findings. For IS, these findings were divided into three main columns: epidermal, dermal and other findings. For ML, benign and malignant cases were mixed and objective findings were evaluated utilizing epidermal, and dermal attributes. The quality of picture was assessed in a scale from 1-3 (1=inferior, 2= similar, and 3= superior quality compared to light microscope). The UHN pathologist was blinded to the clinical information and the final diagnoses.The assessment started with the 20x proceeding to 40x.
Results: The concordance rate for the routine cases scanned from Timmins was (96%). There were 3 minor discrepancies in 3 cases (Intradermal nevus vs. compound nevus, actinic keratosis vs. in-situ squamous cell carcinoma, and seborrheic keratosis vs. verruca vulgaris). These discrepancies were thought to represent judgment bias rather than a function of picture resolution. All the inflammatory skin findings corresponded to the original report except one case where leukocytoclastic vasculitis was originally reported but was not recorded by the UHN pathologist though it was suggested. There was a focus in the original slide that was lost in the scanned recut slide. The 20x scanned slides were given a score of 2 each, however, 40x scanned slides were given a score of 3.The melanocytic lesions showed 100% concordence rate in both the 20x and 40x. However, in malignant and atypical melanocytic lesions 40x gave a superior resolution with detailed nuclear features and easier pick up of mitoses.
Conclusions: Teledermatopathology can serve as a primary and a second opinion diagnostic tool with a potential for expansion to underserviced areas to deliver quality service. Scanning at 40x is superior to 20x particularly in inflammatory and atypical melanocytic lesions.

1715 Gene Expression Profiling of Peripheral Blood during In Vitro Fertilisation Treatment Reveals Predictive Markers of Pregnancy

C Allen, CM Martin, JJ O'Leary. Rotunda Hospital, Dublin, Ireland; Coombe Women's Hospital, Dublin, Ireland.
Background: Infertility is an increasing global disease but the molecular pathways surrounding human conception remain poorly understood. There are no reliable predictors of success for invasive fertility treatments. Here we examine the functional transcriptome in IVF induced pregnancy and non-pregnant controls, to elucidate predictive biomarkers which identify implantation events, maintenance of pregnancy, and pregnancy outcome.
Design: Gene expression patterns in RNA extracted from peripheral blood at time points during IVF cycles from 5 women who achieved clinical pregnancies, 3 women who had implantation failure, and 3 subfertile women who conceived spontaneously